Clim Dyn
DOI 10.1007/s00382-011-1139-5

Comparing modeled and observed changes in mineral dust transport and deposition to Antarctica between the Last Glacial Maximum and current climates

Samuel Albani · Natalie M. Mahowald · Barbara Delmonte · Valter Maggi · Gisela Winckler

Received: 26 November 2010 / Accepted: 28 June 2011

Abstract Mineral dust aerosols represent an active component of the Earth's climate system, by interacting with radiation directly, and by modifying clouds and biogeochemistry. Mineral dust from polar ice cores over the last million years can be used as paleoclimate proxy, and provide unique information about climate variability, as changes in dust deposition at the core sites can be due to changes in sources, transport and/or deposition locally. Here we present results from a study based on climate model simulations using the Community Climate System Model. The focus of this work is to analyze simulated differences in the dust concentration, size distribution and sources in current climate conditions and during the Last Glacial Maximum at specific ice core locations in Antarctica, and compare with available paleodata. Model results suggest that South America is the most important source for dust deposited in Antarctica in current climate, but Australia is also a major contributor and there is spatial variability in the relative importance of the major dust sources. During the Last Glacial Maximum the dominant source in the model was South America, because of the increased activity of glaciogenic dust sources in Southern Patagonia-Tierra del Fuego and the Southernmost Pampas regions, as well as an increase in transport efficiency southward. Dust emitted from the Southern Hemisphere dust source areas usually follow zonal patterns, but southward flow towards Antarctica is located in specific areas characterized by southward displacement of air masses. Observations and model results consistently suggest a spatially variable shift in dust particle sizes. This is due to a combination of relatively reduced en route wet removal favouring a generalized shift towards smaller particles, and on the other hand to an enhanced relative contribution of dry coarse particle deposition in the Last Glacial Maximum.

Keywords Mineral dust · Ice cores · Antarctica · Climate models · Last Glacial Maximum

S. Albani (✉)
Graduate School in Polar Sciences, University of Siena, Siena, Italy
e-mail: samuel.albani@unimib.it

S. Albani · B. Delmonte · V. Maggi
Department of Environmental Sciences, University of Milano-Bicocca, Milano, Italy

S. Albani · N. M. Mahowald
Department of Earth and Atmospheric Sciences, Cornell University, Ithaca, NY, USA

G. Winckler
Lamont-Doherty Earth Observatory, Columbia University, Palisades, NY, USA

G. Winckler
Department of Earth and Environmental Sciences, Columbia University, New York, NY, USA

1 Introduction

Dust suspended in the atmosphere plays a role in the global radiative balance through scattering and absorption of incoming solar radiation and outgoing planetary radiation (Miller and Tegen 1998; Sokolik et al. 2001; Penner et al. 2001; Tegen 2003). In addition dust aerosols can affect cloud nucleation and optical properties (Levin et al. 1996; Rosenfeld et al. 2001). Additional interactions with atmospheric chemistry include heterogeneous reactions and changes in photolysis rate (Dentener et al. 1996; Dickerson et al. 1997). Windblown mineral dust travels long distance

Published online: 09 July 2011

from the source areas and acts as a carrier for nutrients such as iron or phosphorus to remote ocean areas, with implications for biogeochemical cycles and ocean uptake of carbon dioxide (e.g. Martin et al. 1990; Jickells et al. 2005; Wolff et al. 2006; Mahowald et al. 2008).

The most important sources of mineral dust for long-range transport are arid/semiarid regions, with low vegetation cover, located within geomorphological settings prone to accumulation of fine-grained mineral material (Prospero et al. 2002), and with strong winds. After long-range transport, mineral dust can be deposited in different environmental settings; in polar areas, dust is preserved in snow/firn/ice layers, and under favorable conditions it maintains the original depositional sequence forming stratigraphic archives that can be used to study past variations in the dust cycle (e.g. Kohfeld and Harrison 2001). Ice cores revealed a pronounced sensitivity of dust to climate variations both at low latitudes (e.g. Thompson et al. 1995) and in northern and southern polar areas (e.g. Thompson et al. 1981; Petit et al. 1999; Ruth et al. 2003; EPICA Community Members 2004, 2006).

More data is available in the current climate, including in situ concentration data (Prospero and Lamb 2003) or ground based remote sensing data (e.g. Holben et al. 1998; Smirnov et al. 2000). Satellite remote sensing observations provide global insight into worldwide atmospheric dust distributions (e.g. Prospero et al. 2002; Kaufman et al. 2002). Since the early 1990s, dust has been included in global transport models (e.g. Joussaume 1990; Tegen and Fung 1994; Andersen et al. 1998; Mahowald et al. 1999; Ginoux et al. 2001; Werner et al. 2002).

Combining information from paleodust records and climate models in coherent studies can be a fruitful approach from different points of view. For the modeling and present-day observational communities, paleodust records represent a large archive of information on the magnitude and spatial variability of dust deposition for the pre-observational era, and also they represent a target for dust models' validation under different climate scenarios (e.g. Mahowald et al. 2006). In addition, polar snow and firn/ice cores—especially from Antarctica—can act on short (a few years) time scales as collectors for present-day dust that most available techniques currently fail to record, due to the very limited amounts of dust reaching such remote areas (e.g. Bigler et al. 2006; Bory et al. 2010). On the other hand, the understanding of variability in dust transport pathways is fundamental to interpreting ice core dust records. Based on paleoarchives alone it is only possible to compare the spatial variability of dust flux amounts and the geochemical features of the two end-members of the dust life cycle: soil from the potential source areas and dust deposited in ice cores. For this reason physical models are useful tools for studying dust transport patterns. A hierarchy of models has been applied to study aspects related to dust reaching high latitude ice sheets, ranging from simple one-dimensional models (Andersen and Ditlevsen 1998; Fischer et al. 2007) to back-trajectories studies (Lunt and Valdes 2001), to general circulation models (e.g. Genthon 1992; Joussaume 1993; Andersen et al. 1998; Lunt and Valdes 2002a; Werner et al. 2002; Krinner and Genthon 2003; Li et al. 2008; Krinner et al. 2010; Li et al. 2010b).

Here we use an existing, documented model (Mahowald et al. 2006) to look at changes in sources and transport pathways between Southern Hemisphere sources and Antarctica due to changes in climate, and the resulting changes in dust particle sizes and deposition patterns. Our goals are (a) to evaluate the ability of the model to simulate the main physical parameters typical of ice core studies, by comparing them to observations, and (b) to combine information from ice cores and model simulations to make an effort towards explaining the observed changes in dust deposition fluxes and size distributions between the LGM and present climate on a glacial-interglacial timescale. In Sect. 2 we describe the methodology used in the paper. Section 3 shows model results, with focus on dust provenance (Sect. 3.2), transport patterns (Sect. 3.3) and dust size variations (Sect. 3.6), while Sect. 3.4 (dust deposition) and Sect. 3.5 (seasonality) support our discussion. Section 4 discusses our conclusions.

2 Methodology

2.1 Model description

This work is based on simulations performed with the dust model in the Community Atmospheric Model coupled to the Community Land Model (CAM/CLM), which are parts of the Community Climate System Model version 3 (Collins et al. 2006). The detailed description of model setup together with a comparison to observations from the DIRTMAP database (Kohfeld and Harrison 2001) integrated with more recent data from terrestrial sediment records have been published in a previous paper (Mahowald et al. 2006).

The physical model simulations use slab ocean model simulations, and initial conditions are average fields from fully coupled simulations (including atmosphere, land, ocean and sea ice) run until an equilibrium state for current climate and the Last Glacial Maximum (LGM) (Otto-Bliesner et al. 2006; Kiehl et al. 2006). The model has a spectral resolution of T42, corresponding to a horizontal resolution of roughly $2.8^\circ \times 2.8^\circ$ and 26 vertical levels in the atmosphere in the hybrid sigma-pressure coordinate system, with 10–20 tropospheric levels depending at first order on latitude, season and surface elevation. The dust model uses the source entrainment mechanism from

Table 1 Updated/new data used in combination with Mahowald et al. (2006) for the tuning procedure

Site name	Dome C (EDC)	PS2489-2/ODP1090
Longitude	123°21′E	8°58′E
Latitude	75°06′S	42°52′S
LGM/current mass flux ratio	20 (LGM: 18–27 ka BP)	5
Reference	Lambert et al. (2008)	Martínez-García et al. (2009)

Zender et al. (2003) for four size bins (bin1 = 0.1–1.0 μm; bin2 = 1.0–2.5 μm; bin3 = 2.5–5.0 μm; bin4 = 5.0–10.0 μm), and allows for wet and dry deposition (Mahowald et al. 2006). Dust emission in the transport bins has a fixed size distribution partitioning (Mahowald et al. 2006), and dry deposition, more specifically gravitational settling (Zender et al. 2003), is the other process that is directly dependent on the size distribution in the model parameterizations set used for this study. In the set of simulations used for this paper, desert areas change in response to carbon dioxide, temperature, precipitation and insolation changes, using the BIOME3 equilibrium vegetation model (Haxeltine and Prentice 1996). The LGM simulations used here use a tuning procedure to deduce dust source activity in order to include dust mobilization from known glaciogenic deposits (Mahowald et al. 2006). Glaciogenic sources of atmospheric dust correspond to alluvial plains of rivers draining meltwater and fine-grained debris from glaciers and are known to have been active dust sources in the past (e.g. Zárate 2003; Mahowald et al. 2006).

We base this work on 2 sets of simulations, all initialized from equilibrium fields for physical climate: (a) a set of 2 10-years simulations and (b) a set of 13 1-year simulations.

The 10-year simulations (a) consist of one simulation for current climate and one for LGM climate, after a spin up period for dust of 20 and 30 years respectively. With these we will be able to evaluate temporal (inter-annual) variability.

The 1-year simulations (b) start after a 3-months spin up period for dust. The 3-months spin-up period we used for this set of simulations is enough to reach a background equilibrium, considering that (1) estimates of transport times of dust to Antarctica range from a few days to about 2 weeks (Li et al. 2010a; Gassó et al. 2010) and (2) the estimated age of dust deposited to Antarctica is on average 1 month (Han and Zender 2010; Petit and Delmonte 2009).

We have 6 simulations for current climate and 7 for the LGM in which one macro-area at time is active as a source for dust entrainment into the atmosphere (e.g. Mahowald 2007 for current climate; Mahowald et al. 2011 for LGM and current climates). We will use those simulations to study dust provenance. Because here we are focusing on the Southern Ocean and Antarctica, and one of the biggest signals in this region is the large change in the dust between Last Glacial Maximum and current, we tune the model slightly differently than in Mahowald et al. (2006). Dust emission for each macro-area is tuned a posteriori by applying a factor yielding the best fit between the simulated and observed LGM and current deposition rates (as in Mahowald et al. 2006), but we also add the observed LGM/current ratio for dust deposition. For the tuning procedure, we use LGM/current ratios for dust deposition fluxes from a set of observations that includes the observational dataset used in Mahowald et al. (2006) based primarily on Kohfeld and Harrison (2001), integrated with additional data listed in Table 1. The resulting scale factors for each macro-area for both current and LGM climates are included in Table 2. This procedure implicitly assumes that the model atmospheric circulation and geographical location of the source areas are

Table 2 List of model simulations used for the dust provenance study

Macroareas	Current climate			LGM climate		
	Tuning factor	Column dust loading South of 60°S (%)	Dust deposition South of 60°S (%)	Tuning factor	Column dust loading South of 60°S (%)	Dust deposition South of 60°S (%)
Asia (ASIA)	1	<1	<1	1	<1	<1
Australia (AUS)	0.3	21	21	2	10	7
North Africa (NAF)	1	10	1	1	<1	<1
North America (NAM)	1	<1	<1	2	<1	<1
South America (SAM)	1	60	71	1	88	93
Miscellanea (MISC—includes South Africa, East Africa and the Middle East)	1 (S. hemisphere), 4 (N. hemisphere)	9	6	1	2	<1
Europe (EUR)	–	–	–	1	<1	<1

For each one we indicate the tuning factor, and the dust column loading and deposition flux averaged for grid cells South of 60°S, expressed as a percentage of the total, calculated as a sum of results of all simulations, for each climate

Table 3 List of Antarctic ice cores with abbreviations used in this work and geographical location expressed by longitude and latitude

Ice core	Abbreviation	Longitude	Latitude
EPICA dome C	EDC	123°21′E	75°06′S
Vostok	Vk	106°E	78°S
EPICA dronning maud land	EDML	0°E	75°S
TALDICE	Talos	159°06′E	72°49′S
GV7	GV7	158°52′E	70°41′S
Dome Argus	DA	77°22′E	80°S
Dome Fuji	DF	39.4°E	77.2°S
Byrd	Byrd	119°W	80°S
Siple dome	Siple	148°W	81°S
Taylor dome	Taylor	158°E	77°S
Law dome	LD	113°12′E	66°43′S
James Ross Island	JRI	57.7°W	64.2°S
Dome B	DB	94°55′E	77°05′S
Komsomolskaya	KMS	97°29′E	74°05′S
Berkner Island	BI	45°43′W	78°36′S

correct, and forces the magnitude of dust emissions from macro-areas in order to gain a better fit to the observed LGM/current ratio of dust deposition.

2.2 Description of observations

Most of the observations used for the tuning procedure are the same as in Mahowald et al. (2006), and include data from DIRTMAP2 (Kohfeld and Harrison 2001) and other terrestrial records. The only two novelties with respect to Mahowald et al. (2006) are listed in Table 1. Throughout the rest of the work, observations from available ice core sites in Antarctica (Tables 3, 4) are used to compare with model results. In this section we highlight the possible difficulties arising from the compilation of the observational dataset, while those related to model-observation comparison are discussed in the next section. More detailed descriptions of observations are available in the original references (Table 4).

Dust concentration data were obtained using different techniques, depending on the ice core: most are direct measurements of particle concentrations made with either a Coulter Particle Counter or a laser sensor (e.g. Lambert et al. 2008), while other rely on a proxy for mineral dust, such as Aluminum (e.g. McConnell et al. 2007). Dust depositional fluxes, when available, are calculated from concentrations, taking into account the ice/snow accumulation rate of the specific site, which determines the dilution of dust particles in the ice. Multiplying dust concentration (mg dust per kg of ice/snow) times the ice/snow accumulation rate (kg m^{-2} $year^{-1}$) gives the dust depositional flux (mg m^{-2} $year^{-1}$). The snow/ice accumulation rate is subject to some degree of uncertainty due to dating uncertainty and to temporal and spatial variability of snow accumulation, and because of wind-driven post-depositional processes (Frezzotti et al. 2007).

The observationally-derived values of concentration or depositional flux refer to a specific dimensional range of

Table 4 References for observations from Fig. 2

Ice core	Dust concentration/deposition flux	Snow accumulation rate	Observations size range (μm)	Model size range for comparison (μm)
EDC	Lambert et al. (2008)	EPICA community members (2004)	0.7–20	0.1–10
Vk	LGM: Petit et al. (1999). Holocene: dust flux data (Petit J.-R.) from http://www.ncdc.noaa.gov; fluxes have been recalculated assuming a density of 2.5 g/cm^3 for dust. Petit J.-R. (1999): Dust concentration in the Vostok ice core, doi:10.1594/PANGAEA.55502. (Holocene data from the period 0–5.5 kys BP)	Petit et al. (1999)	0.7–20	0.1–10
DA	Xu et al. 2007	Hou et al. (2007)	0.7–5	0.1–5
DF	Miyake et al., AGU Fall Meeting 2007, abstract #PP51A-0199	Kameda et al. (2008)	–	0.1–10
Byrd	Mahowald et al. (1999) and references therein	Mahowald et al. (1999) and references therein	–	0.1–10
JRI	McConnell et al. (2007)	McConnell et al. (2007)	Total–based on Al proxy	0.1–10
BI	Petit J.-R., personal communication (2009)	Debret et al. Geophysical Research Abstracts, Vol. 9, 00807, 2007	0.8–20	0.1–10
Talos	Albani et al. (submitted); Delmonte et al. (2010b)	Frezzotti et al. (2007)	1–5	1–5

dust particles, which may differ depending on the technique and specific instrumental setup. All the ice core data we use here span the 1–5 μm range, which contains most of the dust mass typical of long range transport (e.g. Royer et al. 1983; Delmonte et al. 2002). When possible, we compare model results to the observations in the closest dimensional range (see Table 4).

Measurement uncertainties on each sample are usually low for particle counters (<10%, e.g. Albani et al., submitted), and they are lower then the sample-to-sample (temporal) variability shown by ice core dust records. When using other proxies, the uncertainty may be higher, and only a careful calibration against particle counters may add confidence to the results (e.g. McConnell et al. 2007; Ruth et al. 2008). In this study we use measurements of dust carried out with particle counters, with the exception of the James Ross Island (JRI) data, obtained using Aluminum as a proxy for dust (McConnell et al. 2007).

Observations from the ice cores (Table 4) represent averages of sets of measurements performed on different ice core samples. They typically differ from each other in terms of time integration represented by each sample, time resolution (sampling frequency) and time span of the set of observations for each ice core.

The main differences in time integration and temporal resolution depend on the analysis technique and on the ice accumulation rate at each site (e.g. Masson-Delmotte et al. 2010). These differences can easily be overcome by averaging. The differences in the time span considered is more difficult to reconcile, especially for comparison with the current climate simulations. Apart from JRI, for which we consider the given 19th century average (McConnell et al. 2007), we take dust concentration/flux from averages over the Holocene or sub-periods of the Holocene, depending on data availability. In the case of TALDICE (Table 4) we restricted the time span of reference to the late Holocene (0.8–5 kys BP), although in most cases ice core dust records do not show important trends during the Holocene, compared to the large variability on glacial/interglacial timesacles. This approximation is reasonable considering our approach of comparing equilibrium states for current and LGM climates. When not noted otherwise, observations used in this study were taken from the DIRTMAP2 database (Kohfeld and Harrison 2001).

3 Model results

3.1 Dust flux and concentration: model results versus ice core data

The model is able within a factor 10 to capture the spatial variability of dust deposition globally over four orders of magnitude in both current and LGM climate simulations (Mahowald et al. 2006 and Fig. 1). Estimates suggest that there is an order of magnitude uncertainty in current dust deposition estimates associated with models or observations (e.g. Jickells et al. 2005; Mahowald et al. 2009). Generally speaking, the 10-year simulations and the 1-year simulations used for this study differ in the average total

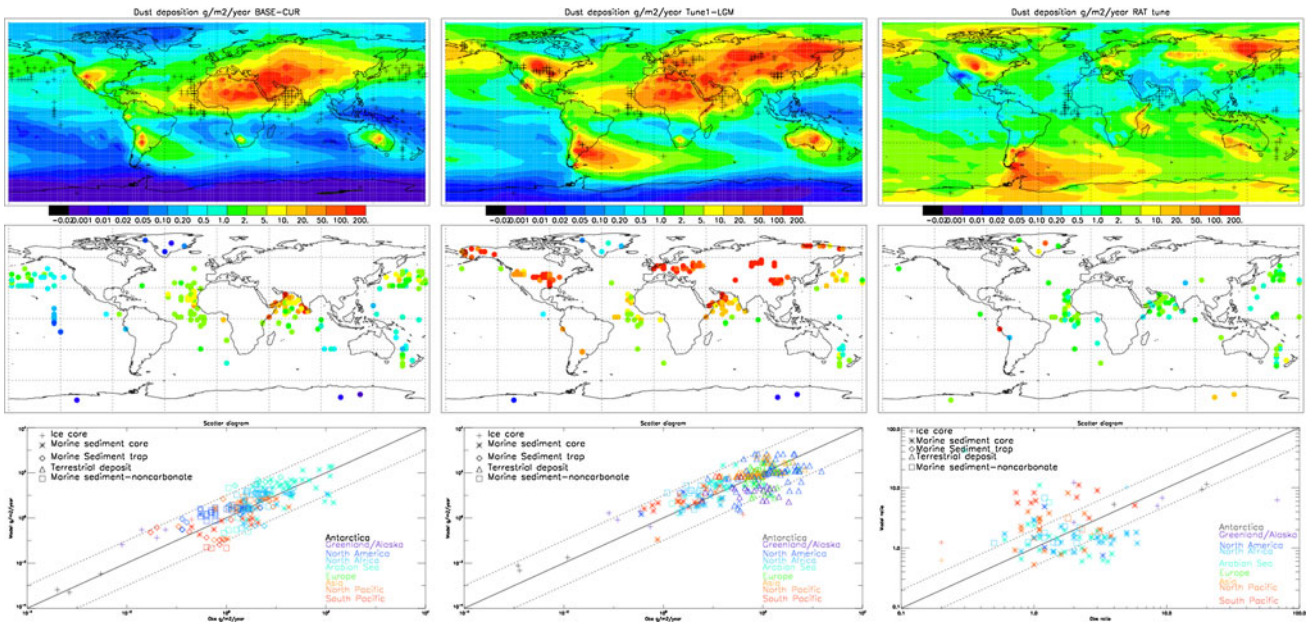

Fig. 1 Dust deposition comparisons between the model (*upper panel*) and observational estimates from DIRTMAP (Kohfeld and Harrison 2001) (*central panel*) and a scatterplot between the model and observations (*bottom panel*). *Left column*: current climate. *Central column*: LGM climate. *Right column*: LGM/current ratio

dust mobilization rate by ~40%, but give similar results in terms of the main aspects analyzed in this study, including seasonality and dust size. The main differences are due to the tuning applied to the source activity in the 1-year simulations, which includes comparison to the magnitude of the glacial-interglacial variations in dust deposition at the observational sites. On the other hand, the number of observations for the LGM/current ratio in dust deposition, and their spatial coverage, is more limited than for individual climate conditions (Fig. 1), and this is a limitation of this approach. In addition, the procedure of calculating a ratio can itself amplify slight mismatches of opposite sign in the model-observation comparison, resulting in higher scatter (Fig. 1). Overall, the model is able to capture much of the observed change in the LGM/current deposition ratio (Table 5).

Now we focus on the Antarctic region, using the data described Table 4. There are two ways to compare observations and model: deposition flux (Fig. 2a, c) or concentration (Fig. 2b, d) in the ice core, and here we show both methods. Note that the model calculates deposition based on precipitation rates and meteorology calculated within the model, and deposition can be converted to ice core concentration by dividing by precipitation rate. Errors of modeled depositional fluxes are comprised of biases in the modeled precipitation (accumulation) rates, as well as errors in the spatial distribution of dust.

Modeled depositional fluxes are compared to observations at different ice cores sites (Fig. 2c). The case-by-case analysis reveals differences ranging within almost zero and a factor of 10 in most cases, depending on the site, variable and simulation. These differences are likely due to uncertainties related to the spatial and temporal variability of measurements, uncertainties related to the snow/ice accumulation estimates based on observations that are reflected in the conversion from dust concentration to flux, to the temporal time window of simulations, as well as to the spatial resolution and biases in the model, discussed below.

Table 5 Average dust mobilization rate (Tg/year) form SAM and AUS from model simulations used in this study (1-year and 10-years simulations, current and LGM climates) and from other relevant works

Simulation	SAM	AUS
1-year (current)	162	59
10-years (current)	168	244
Li et al. (2008) (current)	50	120
Johnson et al. (2010) (current)	33	–
Tanaka and Chiba (2006) (current)	44	106
1-year (LGM)	2,073	422
10-years (LGM)	2,360	236

We see from the set of available observations that the model overpredicts spatial variability in dust fluxes for sites characterized by similar dust deposition (Fig. 2a, c), probably due to biases in modeled precipitation and the associated errors in transport (Fig. 2e). Note that our model overpredicts the wet versus dry deposition rates in Antarctica (Mahowald et al. 2011), possibly amplifying biases in precipitation. Here the relatively coarse spatial resolution of the model may prevent fully capturing the changing slopes at the edges of the ice sheets, causing biases in moisture transport inland and precipitation rates. Similar findings were discussed in previous modeling studies (Delaygue et al. 2000; Noone and Simmonds 2002).

Mahowald et al. (2011) use a correlation technique using the same model as here to estimate whether at a given location deposition or concentration is more representative of dustiness and deposition. In contrast here we compare to available data for both deposition and concentration. In this case, modeled concentrations compare better to observations than deposition fluxes, perhaps because this reduces the biases from errors in precipitation rates. This highlights the problem with simulating dust deposition well: in order to get a more realistic representation of the spatial variability of dust fluxes, the model needs to capture precipitation correctly as well, which is not achieved in climate models.

3.2 Dust provenance

3.2.1 Model results

Here we present results from two sets of 1-year simulations using just one dust source area at a time for current climate and for the LGM (Table 2). All sources worldwide grouped in macro-areas roughly corresponding to the continents (Table 2) are considered, and for present-day climate there are two major dust sources in the Southern Hemisphere, namely Australia (AUS) and South America (SAM), and we consider both the column loading and the deposition. SAM is the dominant source in the LGM. We highlight possible interhemispheric dust transport, although the minor sources from North Africa contribute even less to dust deposition than loading (Table 2). Similar results for inter-hemispheric transport were seen in Li et al. (2008). The comparison among modeled dust mobilization rates from SAM and AUS from different works (Table 5) shows that the relative magnitudes vary from case to case. Relatively high values from our simulations depend largely on the size distribution imposed, with most of the mass in the coarser bin readily removed close to the source areas (Mahowald et al. 2006). In the 10-year simulations the AUS is larger than the SAM source, but in the 1-year

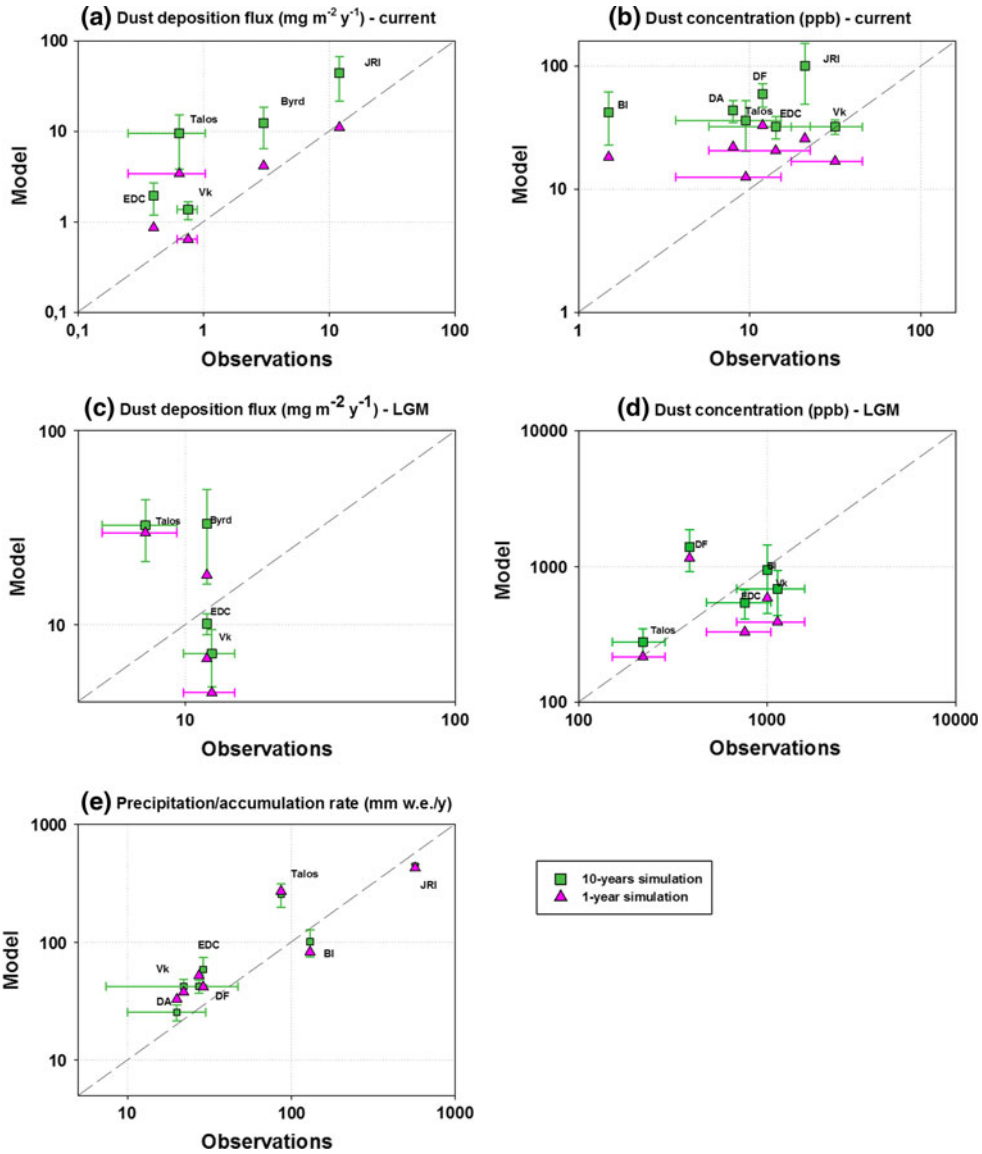

Fig. 2 Comparison of model outputs versus observations from 2 different sets of simulations. **a** Dust deposition flux in current climate. **b** Dust concentration in ice cores in current climate. **c** Dust deposition flux in LGM climate. **d** Dust concentration in ice cores in LGM climate. **e** Modeled precipitation versus observed snow accumulation rate in current climate

simulations the tuning factors (Table 2) result in a reduction in AUS source so that SAM is larger.

In Fig. 3 the relative contributions to deposition from the main sources, is shown for both current climate and for the LGM (the total deposition is shown in Fig. 1). Two main features are evident. First, each of the two most important sources (SAM and AUS) tends to dominate the region directly downwind from the source, as expected; second, SAM is the dominant source for dust deposited all over Antarctica in both climates, as seen in Table 2. Still, especially in the current climate simulation, AUS is an important contributor in Victoria and Adélie Lands (East Antarctica), West Antarctica and the Antarctic Peninsula. The regions which are dominated by SAM tend to be downwind of South America (Fig. 3a), and this region grows in the LGM (Fig. 3b).

3.2.2 *Comparing model results with observations: current climate*

From an observational point of view, the study of dust provenance relies mainly on the comparison between the geochemical composition of dust retrieved from ice cores and target samples from the potential source areas (PSA). One of the most commonly used geochemical tracer is the Nd and Sr isotopic composition of dust, which is an intrinsic property of dust, conservative from the source to the sink (e.g. Grousset and Biscaye 2005). More recently, new isotopic and elemental composition systems (e.g., Pb, Li, He isotopes) have been utilized to fingerprint geochemically the dust (Vallelonga et al. 2010; Gabrielli et al. 2010; Marino et al. 2008; Winckler and Fischer 2006; Siggaard-Andersen et al. 2007); yet, geochemical data

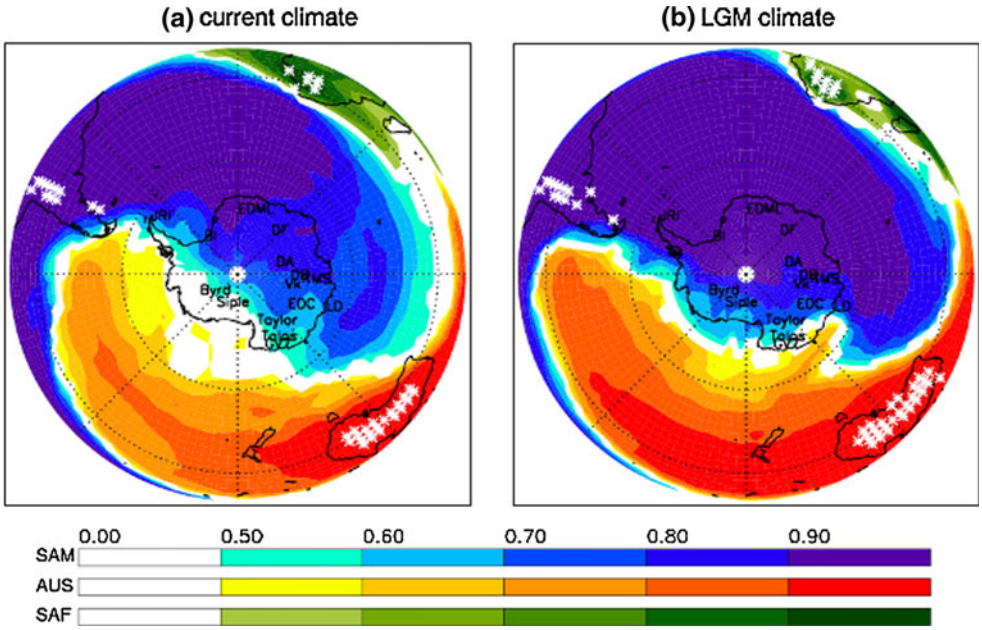

Fig. 3 Maps for source apportionment in dust deposition, represented by the relative fractions to the total deposition flux, of dust originated from South America (*blue color scale*), Australia (*red color scale*) and South Africa (*green color scale*). *Colored areas* indicate that at least half of the deposited dust was originated from the corresponding macro-area. *White stars* represent active sources for dust mobilization. **a** Current climate. **b** LGM climate

available for interglacial dust, mostly from the Holocene or the previous interglacial period (MIS 5.5), is still limited.

There is increasing consensus that dust deposited in Antarctica during interglacial time periods is derived from a mixture of dust sources rather than a single source. Potential sources include different regions within southern South America and other sources like AUS (Revel-Rolland et al. 2006; Delmonte et al. 2007) or possibly the Puna-Altiplano area (Delmonte et al. 2008a; Gaiero 2008), and match the limited data on the isotopic signature of interglacial dust from the studied ice cores. A Holocene mixture of SAM and AUS dust for central East Antarctica is also supported by the dust elemental composition (major elements: Marino et al. 2008). On the other hand, lead isotopic composition on dust from EPICA Dome C (EDC) indicates Australia as a minor source (Vallelonga et al. 2010), but other studies (e.g. Vallelonga et al. 2010; Gabrielli et al. 2010; Lanci et al. 2008) suggest that a contribution from local Antarctic sources must be also taken into account. For peripheral Antarctic sites such as Talos Dome (Delmonte et al. 2010b; Albani et al. submitted) and Berkner Island (Bory et al. 2010), moreover, preliminary results suggest a contribution from local Antarctic sources during the Holocene and present-day. Note that the model does not consider local sources of dust.

The simulated contribution of South African dust to the deposition budget in Antarctica (Table 2) is significant only in current climate conditions in peripheral East Antarctica between 45°E and 120°E (not shown), where it is more important than AUS; however, they both represent minor contributors there compared to SAM. Possible importance of SAF dust contributions to East Antarctica seems unlikely, and the only observations close to the indicated sector are from Law Dome and they rather indicate contributions from AUS (Burn-Nunes et al. 2011).

In summary, the results from our modeling study agree with the observationally based studies suggesting AUS significantly contributing to the dust deposition budget in central East Antarctica in current climate conditions (Fig. 3a). As previously stated the model does not include Antarctic sources in the simulations performed, so no comparisons are possible with these observationally-based hypotheses.

In the model simulation, active dust sources in SAM are located North of 32°S, corresponding to the Western Argentinean Loess (W-ArL) and the Andean Puna-Altiplano plateau, while active sources in Central-Eastern Patagonia lying between 45°S and 50°S, provide a negligible contribution to the total SAM dust mobilization budget. The model is able to capture the location of the main dust sources in South America (Prospero et al. 2002), but the magnitude and relative proportions of source areas are difficult to evaluate. Yet, the small proportion of dust mobilization from Patagonia in our simulation may be an underestimation (Prospero et al. 2002), since observations report dust plumes in this region (e.g. Gassó and Stein 2007; Li et al. 2010a; Johnson et al. 2010). A recent study showed that dust mobilized from the same latitude band in coastal Patagonia is able to reach Antarctica at present, as well as from Tierra del Fuego (Gassó et al. 2010). In this study we did not track dust coming from different parts of SAM, and specific sub-regional source activity is not necessarily proportionally correlated with the total SAM dust budget above Antarctica, because of the complexity of transport patterns.

At first order our results for dust provenance during current climate qualitatively agree with previous work, in

terms of identifying SAM in general as the most important source for Antarctica (Andersen et al. 1998; Lunt and Valdes 2001, 2002a). If we focus on the relative proportions of dust mobilization within SAM sources, our study is similar to Andersen et al. (1998), but does not agree with Lunt and Valdes (2002a). The spatial distribution of areas dominated by either SAM (as a whole) or AUS dust is qualitatively similar to Li et al. (2008), although large differences exist in the relative proportions of the simulated dust emission from different sub-areas within SAM (e.g. Patagonia vs Altiplano or Cordoba region), that may render the comparison difficult because of different efficiencies in transport.

3.2.3 Comparing model results with observations: LGM

For the LGM the geochemical fingerprint of dust from central East Antarctic ice cores (Vostok, old Dome C, Dome B, Komsomolskaya, EPICA-Dome C and Talos Dome) shows a dominant South American provenance for dust (e.g. Grousset et al. 1992; Basile et al. 1997, Delmonte et al. 2004b, 2008b, 2010a), in agreement with the model outcomes presented in this study (Fig. 3b) and with previous studies (e.g. Genthon 1992; Andersen et al. 1998; Lunt and Valdes 2002a; Krinner and Genthon 2003). The two most active grid cells in the LGM simulation (Fig. 3b) are located between 37°S and 42°S, roughly corresponding to the southernmost Pampas, specifically the Rio Colorado and Rio Negro basins. Samples from those regions have a typical Patagonian isotopic signature (Gaiero et al. 2007), which means that the model generally agrees with observations. The model also shows a weaker source in southernmost Patagonia (S-Pat)—Tierra del Fuego (TdF). Isotopic data for the TdF are still very scarce (Sugden et al. 2009), preventing any firm conclusion on the importance of that area. The sources from the Pampas region were explicitly accounted for as a glaciogenic source for dust in the LGM, based on Zárate (2003) (Mahowald et al. 2006).

Other active but relatively weak sources in the simulation for the LGM include the Westren Argentinean Loess (W-ArL) flanking the Andes North of 32°S and the Puna-Altiplano in the Andean cordillera (Fig. 3b).

3.3 Transport patterns

3.3.1 Current climate

Spatial features of dust loading and transport in the Southern Hemisphere, together with implications for dust provenance, are examined in this section. A more detailed discussion of winds in Community Climate System Model version 3 (CCSM3) is given in Otto-Bliesner et al. (2006). We also qualitatively checked winds from both 1-year and from long-term runs against fully-coupled CCSM3 zonal winds (Rojas et al. 2009), confirming a good agreement, especially for the lower levels. Simulated winds capture the general features of atmospheric circulation above Antarctica (e.g. King and Turner 1997; Parish and Bromwich 2007).

Dust advection in the atmosphere is controlled by the general circulation and disturbances on a synoptic scale (e.g. Li et al. 2010a). Here we analyze climatological features on a seasonal basis, as simulated by the model. Simulations for the current climate show a latitudinal gradient in SAM dust loading, with a minimum over Antarctica, that varies with altitude and season (Fig. 4), similarly to the case of the AUS source (not shown). Dust is preferentially advected around Antarctica within the Westerlies over the Southern Ocean, and the latitudinal gradient is more pronounced for lower levels (950 mb) compared to the higher ones (650 and 500 mb). The higher altitudes show a larger dust loading at all latitudes, suggesting that transport preferentially takes place in the mid-high troposphere (Figs. 4, 5). This is consistent with the ice sheet and the corresponding high pressure system acting as a barrier to the southward-moving air in the lowest levels of the atmosphere (Parish and Bromwich 2007).

The analysis of vertical profiles of source-apportioned dust loading above specific sites (EDC: Fig. 5; similar to EDML and Talos, not shown) confirms the seasonal variations in dust loading, with seasonal differences more or less pronounced depending on the site. A common feature of vertical profiles from either SAM or AUS in the current climate is the presence of a double peak of dust loading in vertical height (also Fig. 6c); the presence and height of this relative maximum depends on season and location. A common characteristic of all Antarctic sites investigated is a spring (SON)—to-summer (DJF) maximum and a winter (JJA) minimum in dust concentrations aloft.

Because of the nature of the hybrid sigma-pressure vertical coordinate used in the model, grid boxes at the same vertical level do not necessarily have the same elevation above sea level, especially in the lower levels (Washington and Parkinson 2005). More important for transport, parcels of air do not follow the vertical model layers but rather tend to stay on the same level of neutral buoyancy (potential temperature). Thus horizontal transport patterns (and winds) would not necessarily follow trajectories lying at the same vertical level in the coordinate system. Interpolating to a pure pressure vertical coordinate helps visualizing vertical profiles of dust, although even in this case the difference between elevation above sea level and the model vertical grid will be more important when adjacent surface grid cells are characterized by large elevation (orography) gradients (Fig. 6).

Comparing our results with those from Li et al. (2008), some differences arise, especially in terms of vertical

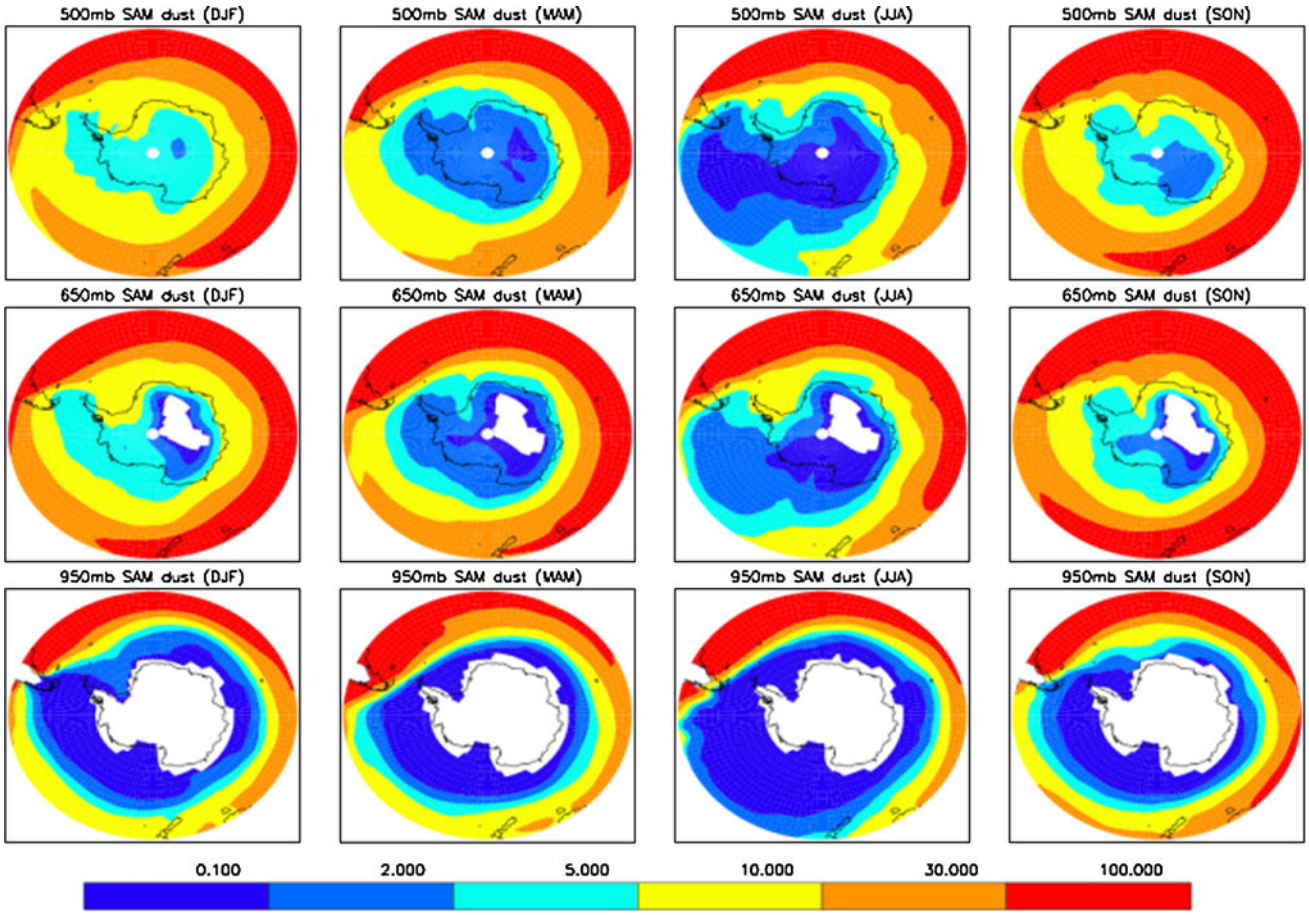

Fig. 4 Seasonal evolution of dust loading (*colors*, [μg/m^2]) at three different vertical levels, for SAM dust in current climate. Each *row of maps* represents a different vertical level, in the pressure vertical coordinate. From the *top*: 500 mb, 650 mbar and 950 mbar. Each column of maps represents a different season. From the *left*: summer (DJF), fall (MAM), winter (JJA) and spring (SON)

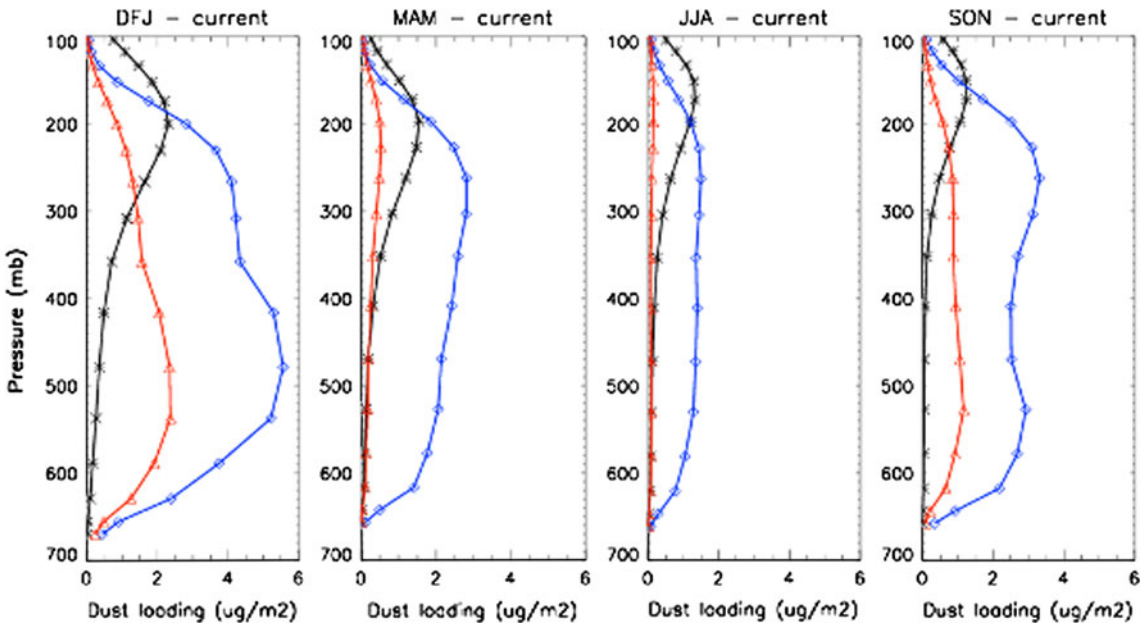

Fig. 5 Seasonal evolution of vertical profiles of dust loading over Dome C, simulated for the current climate from different sources (*blue* = SAM, *red* = AUS, *black* = NAF). From left to right plots for the different seasons: summer (DJF), autumn (MAM), winter (JJA) and spring (SON)

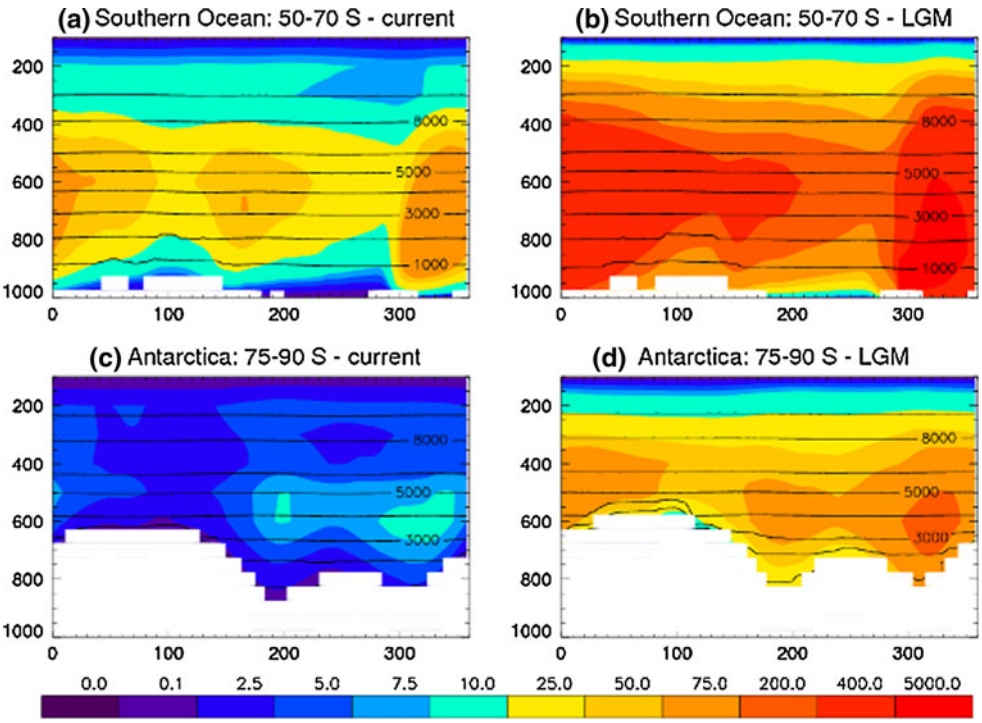

Fig. 6 Vertical profiles of dust loading ($\mu g/m^2$) averaged over two distinct latitudinal bands (Southern Ocean: 50°–70°S; Antarctica: 75°–90°S), in function of longitude (*x*-axis) and pressure (*y*-axis). *Black lines* represent the height (m above sea level) of correspondent pressure levels. **a** Southern Ocean, current climate. **b** Southern Ocean, LGM. **c** Antarctica, current climate. **d** Antarctica, LGM

distribution of dust. For the SAM source, part of the difference may be explained by different location of the active source areas. These are focused in Patagonia for Li and coauthors, but more broadly located in the W-ArL, the Altiplano and Patagonia for this study. In particular, the Patagonian source is at much higher latitude compared to the other SAM sources, and has very stable atmospheric conditions (Li et al. 2008, 2010a). Dust originated from Patagonia is transported in the boundary layer before being uplifted by low pressure system moving eastward over the Southern Ocean (Li et al. 2008, 2010a). On the other hand, the Altiplano source is at high elevation and dust will be transported in the free troposphere, and in out model also dust from W-ArL (the major simulated source) is uplifted close to the source areas. Patagonia is active in our simulations for current climate, although quantitatively the dust mobilization is very modest. Despite its low activity in our simulation, Patagonia could still have the potential be an important source for dust transported Southward, because of transport efficiency. This fact has been suggested from combined satellite observations and models that show dust plumes from Patagonia are able to travel long distance reaching the sub-Antarctic Atlantic Ocean (Gassó and Stein 2007) and even Antarctica (Gassó et al. 2010).

3.3.2 LGM climate

Changes in transport patterns between current climate and the LGM have been analyzed in order to understand their role in dust deposition changes and to analyze their relationship with observed and modeled changes in dust provenance. The analysis of vertical profiles for dust loading for both meridional averages (Fig. 6) and specific sites for dust of different origin (analogous to Fig. 5, not shown) highlights the generalized feature of uni-modal vertical distributions (in contrast to the bimodal vertical distribution in the current climate) with seasonal peak shifts in the vertical profile. Some sites still show a weakly pronounced double peak as seen in current climate simulations. The characteristic uni-modal peak tends to be located at lower levels than the most prominent lower peak typical of current climate simulated vertical profiles (see also Sect. 3.6.2 for further details). This is consistent with a colder climate having colder surfaces and less strong vertical mixing, and was seen in the zonal mean concentrations distributions (Mahowald et al. 2006).

The analysis of atmospheric dust loading at different levels and seasons for SAM dust in the LGM (Fig. 7), reveals a picture broadly similar as the current climate (Fig. 4). The main difference, besides the magnitude of dust loading, is the more marked transport pathway with a dust plume connecting Patagonia to the Antarctic Peninsula/Western Antarctica (Fig. 7i, l). This is consistent with modeled shift in wind directions (with more southerly flow in the LGM) around 280°E, also noticeable from simulated glacial/interglacial variations in winds stress (Otto-Bliesner et al. 2006). At present day dust can be advected from Patagonia towards Western Antarctica under certain synoptic conditions, although the prevalent transport patterns are directed towards East Antarctica (Li et al. 2010a). Our

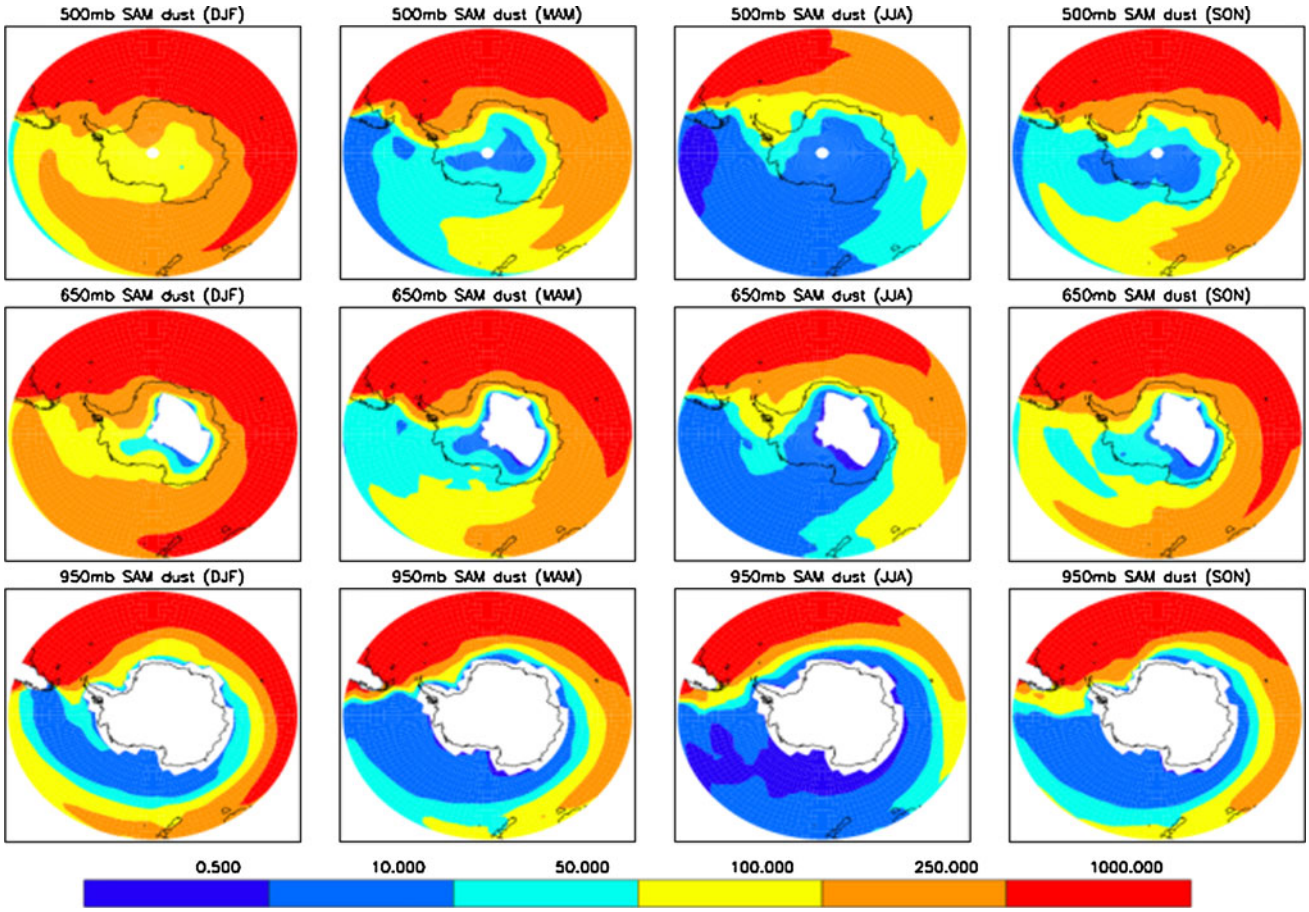

Fig. 7 Same as Fig. 4 in the LGM climate simulation

model results suggest that a variation during the LGM of the prevalent meteorological conditions (on a seasonal basis) around the Drake Passage area in the Southern Pacific and Atlantic Oceans would allow a more frequent direct advection of dust towards the Antarctic Peninsula/West Antarctica from South America (see next section). Modifications in transport pathways to West Antarctica during the LGM related to circulations effects, in particular to a increase in southward winds west of the Drake Passage, have also been suggested by Li et al. (2010b).

3.3.3 Preferential areas of access

Next we consider how dust is brought to Antarctica, according to the model. Meridional transport of dust towards Antarctica is controlled by eddies in the Southern Ocean on a synoptic scale (Li et al. 2010a). SAM dust penetrates southward more efficiently in the Dronning Maud Land (DML) area, in particular around 350°–360°E and 30°–40°E (Fig. 4). We see this from the relatively high concentrations of dust, compared to other longitudes at the same latitude. This is true for all atmospheric levels considered and is variable with seasons, being strongest in spring/summer (SON/DJF). Interestingly, Parish and Bromwich (2007) point to those longitudes as to areas characterized by preferential southward transport of air masses, consistent with the winds predicted in the model. Ice topography is a major factor in controlling the atmospheric circulation in the lower levels with effects extending nearly 2 km above the surface, associated with the stationary wave forced by the Antarctic continent. It results in low-level exchanges of mass between the high southern latitudes and the rest of the atmosphere that are concentrated in specific locations, where the terrain departs markedly from zonal symmetry (Parish and Bromwich 2007).

Similar analysis shows that preferential pathways for transport southward for AUS dust (not shown) are evident for spring (SON) and summer (DJF), located mainly on the Western side of the Ross Sea and at longitudes around 270°–300°E, at ~650 and ~500 mb. At lower levels the same zonal bands were also identified as southward transport zones for air masses by Parish and Bromwich (2007) and agree with our wind vectors. At higher altitudes the southward transport of air masses and dust around 270°–300°E is coherent with the cyclonic circulation

centered above the Ross Sea (e.g. Parish and Bromwich 2007). Additional access points for AUS dust are Western Antarctica in general, the Weddell Sea and Western DML.

The meridional southward advection of dust through preferential pathways associated with air masses exchange between Antarctica and lower latitudes (the climatological expression of synoptic scale disturbances that control meridional transport), and subsequent entrainment into the anticyclonic airflow over the continent, causing mixing and redistribution of dust all around Antarctica, is consistent with observational evidence based on ice cores suggesting rather uniform characteristics of dust deposited over the Atlantic and Indian sectors of the Eastern Antarctic Ice Sheet (Ruth et al. 2008), at least for the LGM (Marino et al. 2009).

Other modeling studies pointed out important features we described such as zonal advection of dust around Antarctica, with Australia being—at least in some sectors—a major dust source for current climate (Andersen et al. 1998; Li et al. 2008; Krinner et al. 2010), and preferential access points to the Antarctic interior: the Ross Sea sector (Andersen et al. 1998), Dronning Maud Land and West Antarctica (Krinner et al. 2010). Here we suggest a comprehensive picture of the spatial distribution of enhanced meridional transport areas and the general features of Antarctic atmospheric circulation, and how that changes between current and LGM climate.

Concerning dust lifetimes, as noticed above, it is relevant that the model simulates dust lifetimes longer than 30 days above the interior of the East Antarctic Plateau (Fig. 8). Given that in this study we are not assessing dust transport times themselves, we stress how the discrepancy between suggested transport/transit time in the literature may be related to the conceptual difference in the diverse approaches that have been used to assess this problem. Dust can be both transported to Antarctica in less than 2 weeks (Krinner and Genthon 2003; Li et al. 2010a) and still not be deposited in central East Antarctica before a month (Petit and Delmonte 2009). Lifetime is the relevant parameter used in the latter study, and seems in line with our model simulations, but this is something different than the transport time itself (Han and Zender 2010).

3.4 Dust deposition

3.4.1 LGM/present-day ratios of dust loading and deposition flux

In this section we focus on the ratio of LGM to current dust observed in the paleorecords, and how these are simulated in the model. An increased mobilization rate from the source areas is reflected in increased dust loading (e.g. Fig. 6) and deposition (Fig. 1). While the simulated global average for the LGM/current deposition ratio is $\sim$2.4, larger values than this are evident. Specific variations in source areas relevant for this study ($\sim$7 for AUS and $\sim$ 13 for SAM in the LGM/cur tuned 1-year runs; $\sim$1 and $\sim$14 respectively from the average of the 10-years simulations) are also reflected over large areas of globe in both dust loading (not shown) and deposition (Fig. 1). In particular higher values are present in correspondence of the main LGM-enhanced dust corridors, with declining gradients towards their edges (see also Mahowald et al. 2011). This suggests that spatial variability is important when considering the LGM/current deposition ratios.

A map of lifetime of mineral dust (Fig. 8a–c) suggests a generalized slight increase in dust lifetimes over large areas of the Southern Ocean, possibly linked to the reduced

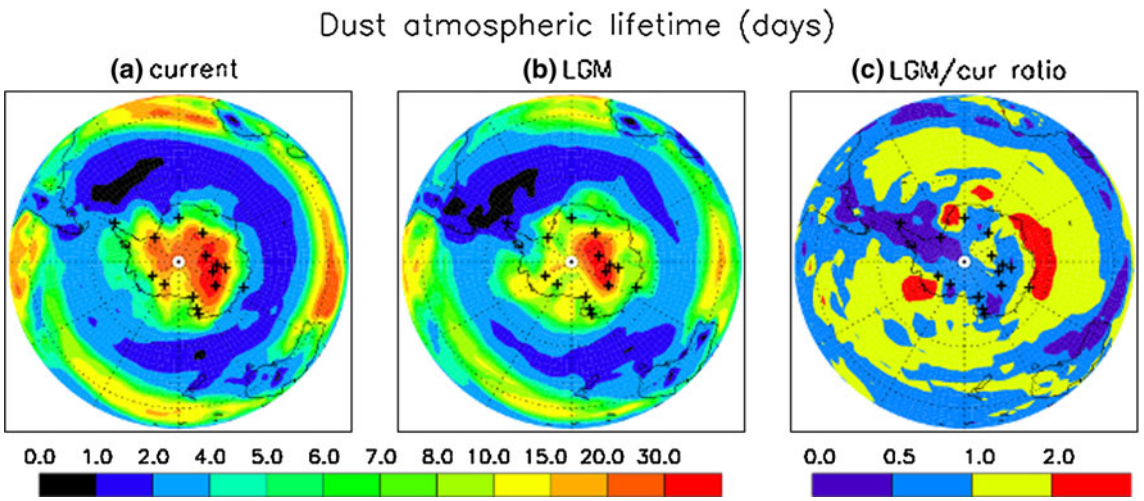

Fig. 8 Dust atmospheric lifetimes (days), calculated as a ratio between dust loading and deposition ratio at each grid cell. **a** Current climate simulation. **b** LGM climate simulation. **c** LGM/current ratio

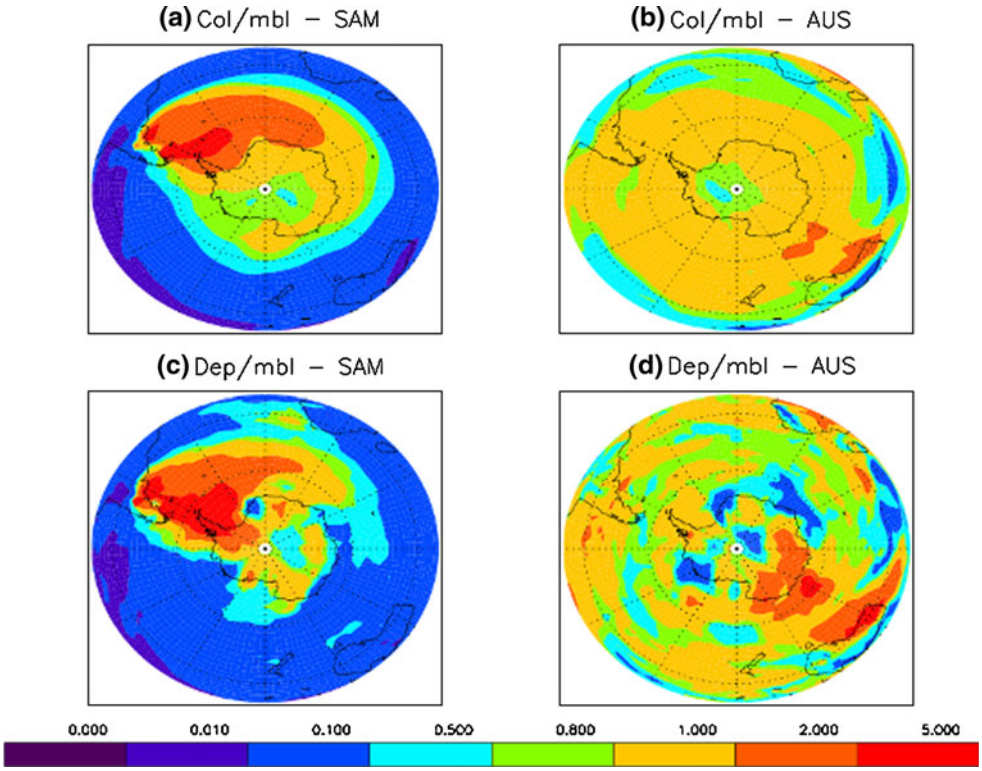

Fig. 9 Maps for the LGM/current ratio of transport efficiency, defined as the ratio between either column loading (**a**, **b**) or deposition rate (**c**, **d**) at each grid cell (separately for SAM and AUS dust) and total dust mobilization rate from the source area (SAM or AUS)

precipitation frequency, in accordance with long-term CCSM3 simulations (Rojas et al. 2009; Mahowald et al. 2011). Precipitation frequency appears more important that total precipitation for wet deposition lifetime (see discussion in Mahowald et al. 2011). Interestingly, a decrease in lifetimes is evident in large areas over Antarctica (with the exception of the interior of central East Antarctic plateau). This is likely to be related to the lower levels of the dust transported to Antarctica (see above). An increased transport efficiency from the source areas is clearly evident for SAM (Fig. 9a, c), though not for AUS (Fig. 9b, d).

To explain the high LGM/current deposition ratios, the importance of additional dust sources in the LGM at high SAM latitudes $>\sim 40°S$ was suggested by Andersen et al. (1998), together with the increased low level transport from Patagonia favored by the increased cyclonic activity in the Weddell Sea (Krinner and Genthon 1998; Andersen et al. 1998; Krinner and Genthon 2003). Here we show (Fig. 9a, c) that the model predicts that (southward) latitudinal displacement of SAM dust sources in the LGM, possibly in combination with changes in transport, is important in explaining the large increase in dust deposition. This combination of factors are consistent with the hypothesis that there is enhanced coupling between Antarctic climate with that of the Southern Hemisphere mid latitudes during glacial periods relative to interglacials (e.g. Petit et al. 1999; Lambert et al. 2008). Present-day studies have highlighted the increasing efficiency of dust transport from southern sources of dust versus those farther north in Patagonia (Gassó et al. 2010; Li et al. 2010a). Possible underestimation of present-day dust emissions from Patagonia in our simulation may enhance the simulated LGM/current variability described here. The conclusions on increased efficiency for more Southern source areas remain qualitatively similar.

The increased dust transport efficiency in the LGM (including more direct transport to the Antarctic Peninsula/West Antarctica: Fig. 9a, c, Sect. 3.3.2) is particularly enhanced at lower levels, but detectable throughout the troposphere, and possibly prevents the splitting of dust pathways in the vertical level seen in the current climate simulations (Fig. 6). This split may be just an artifact, but probably results from averaging several dust events either from different sources or with different pathways. The lower transport pathway in the LGM also results in higher values of deposition compared to loading over Antarctica (compare Fig. 9a, c), consistent with the idea that the lower vertical distribution of dust makes it more easily removed by both wet and dry deposition processes (see Sect. 3.6.2). It is noteworthy to stress that while differences in latitude and elevation of the SAM source areas—such as those between this work and e.g. Li et al. (2008)—may affect the vertical level of transport downwind of the sources themselves, once dust-carrying air masses are entrained in the atmospheric circulation over the East Antarctic Plateau the air masses will be well mixed.

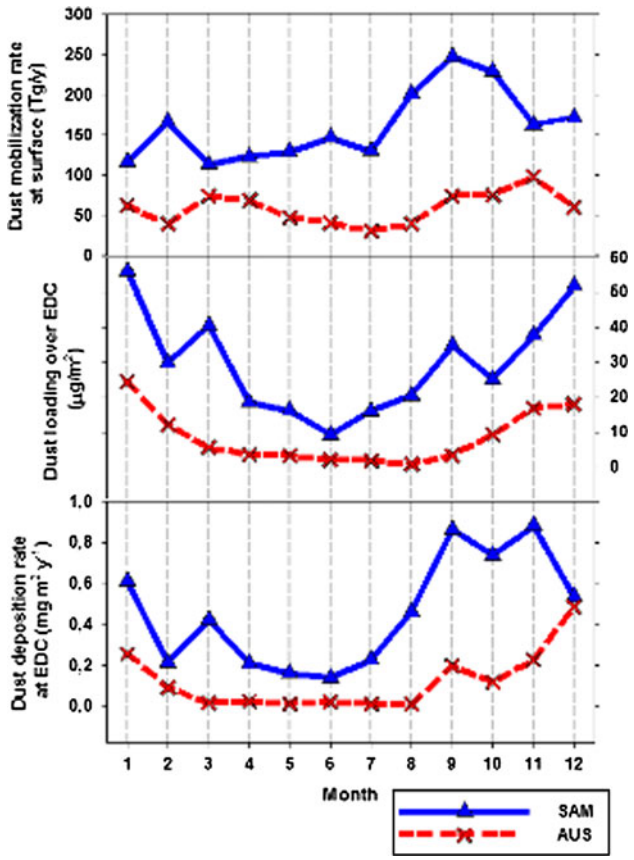

Fig. 10 Annual cycle for simulated dust mobilization (from SAM and AUS), loading (over Dome C) and deposition (over Dome C), for current climate. *Blue solid line* with triangle marks is SAM, *red short-dashed line* with crosses is AUS

So several mechanisms likely work together to produce the higher dust deposition in the LGM: larger dust mobilization, enhanced transport efficiency from Southern Patagonia, less vertical mixing (see also Mahowald et al. 2006), less wet deposition removal en route and more efficient scavenging over Antarctica, due to lower transport levels.

3.5 Seasonality

Here we briefly review the seasonal signals described throughout the work in comparison with observations, to check the consistency of our results.

3.5.1 Seasonality: dust mobilization and transport

Modeled dust mobilization from SAM (Fig. 10) shows a clear peak during the austral spring (SON), in agreement with observational data for dust mobilization in SAM (Prospero et al. 2002; Gaiero et al. 2003). AUS dust mobilization is predicted in the model to peak in autumn (MAM) and keep high during winter (Fig. 11), while observations suggest a more pronounced annual cycle at its top during winter months (McTainsh and Lynch 1996; Prospero et al. 2002).

Modeled seasonal variations in dust concentration and optical depth have previously been evaluated, and are not fully able to capture the observed variability, which is due to either the biases in precipitation and winds in the physical model, or to errors in the dust source and deposition algorithms (Mahowald et al. 2006). Here we plot comparison of surface concentrations for 3 sites (Fig. 11a), showing underestimation of the magnitude for all sites, while in general our model performs better for dust deposition (e.g. Figs. 1, 2). Possible causes include underestimation of dust mobilization from Patagonia and/or biases in vertical mixing in the lower levels of the troposphere.

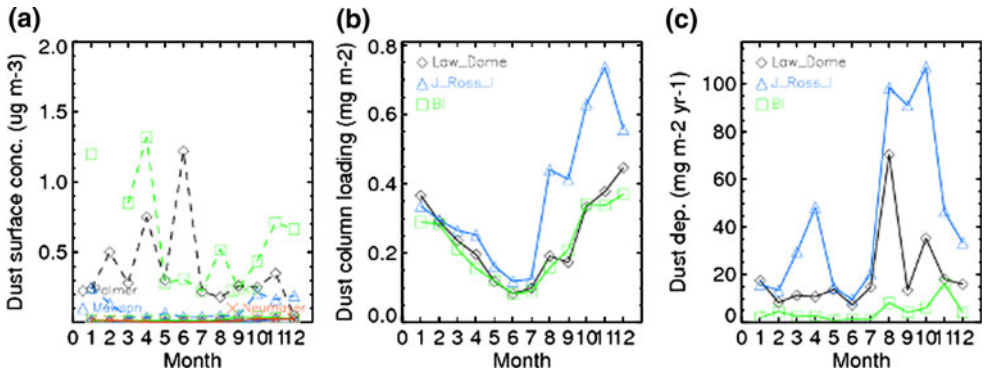

Fig. 11 Time series of monthly averages for dust surface concentration (μg/m^3), dust column loading (mg/m^2) and dust deposition (mg m^{-2} year^{-1}) at different sites, from the 10-years simulation. **a** Dust surface concentrations simulated (*solid lines*) at Palmer (64.77°S, 64.05°W; *black*, *diamonds*), Mawson (67.60°S, 62.50°E; *blue*, *triangles*), Marsh-King George Island (KGI) (62.18°S, 58.30°W; *green*, *squares*) and Neumayer (70°39′S; 8°15′W; *red*, x), compared with observations (*short-dashed lines*) from the University of Miami Ocean Aerosol Network. **b** Dust column loading simulated at Law Dome (*black*, *diamonds*), James Ross Island (*blue*, *triangles*) and Berkner Island (*green*, *squares*). **c** Dust deposition flux simulated at Law Dome (*black*, *diamonds*), James Ross Island (*blue*, *triangles*) and Berkner Island (*green*, *squares*)

Simulations (Fig. 11a) show agreement for the seasonal cycle at Mawson, but not at Palmer nor (for the limited observations available) at King George Island. Previous works also showed simulated summer maxima agreeing with observations at Mawson (Lunt and Valdes 2002b; Tanaka and Chiba 2006; Li et al. 2008), but not at Palmer (Lunt and Valdes 2002b). In addition we show (Fig. 11a) the simulated average annual cycle of dust surface concentration at Neumayer, that shows spring/summer maxima and winter minima, in agreement with the main seasonal cycle of Lanthanum-based observations (Weller et al. 2008). Summer maxima were clearly identified from aerosol sampling at South Pole, Neumayer Station and the Antarctic Peninsula (Cunningham and Zoller 1981; Weller et al. 2008).

For the current climate simulations, the seasonal pattern of dust loading around and above Antarctica for both SAM (Figs. 4, 5) and AUS is higher in spring (SON) and in summer (DJF) with winter (JJA) minima, visible also from a selection of specific sites on the margins of Antarctica (Fig. 11b). In autumn (MAM), despite the relatively high mobilization rate for AUS (Fig. 10), dust transport towards high latitudes is not maximum (Fig. 4), suggesting that transport impacts the seasonal cycle of dust over Antarctica.

Winter and spring storms transport heat, and constituents towards to the polar regions. On the Antarctic continent, while surface wind directions in summer differ only slightly from that observed during the winter, wind speeds display pronounced seasonal differences, showing winter maxima. Therefore, as the continent cools, drainage flows intensify and northward low-level mass fluxes from Antarctica increase. This results in an overall summertime air mass loading and in a wintertime mass transport away from the edges of Antarctica, counterbalanced by broad subsidence occurring over the continent (Parish and Bromwich 2007).

3.5.2 *Seasonality: dust deposition*

A seasonal cycle is evident for dust loading, and less pronouncedly also for dust deposition flux (Figs. 10, 11b, c). The picture is qualitatively similar for all ice core sites analyzed. In the case of LGM simulations we still have a seasonal cycle, though less well-defined, especially in the case of dust deposition (not shown).

We compare our results (Figs. 10, 11c) to the limited observations. Direct observations of dust deposition in Antarctica are very difficult because of the very low atmospheric concentrations and deposition rates (Bigler et al. 2006). Although the first observations of seasonal cycle in dust concentrations suggested winter peaks (Thompson 1975) later studies questioned this first evidence (Thompson 1977; Mumford and Peel 1982 and references therein). Winter deposition maxima were also suggested later, based on non-sea salt calcium proxies with large uncertainties (Sommer et al. 2000). Recently it was shown, based on trace metals analysis, that the dust depositional annual cycle at Law Dome shows spring and autumn maxima and winter minima (Burn-Nunes et al. 2011), while our simulation indicates winter minima in June followed by late winter/spring maxima (Fig. 11c). Similarly, our model simulates late winter/spring maxima at JRI, quite similar to Aluminum-based observations indicating the peak season in late winter (McConnell et al. 2007). A clear seasonal cycle has been recently observed from snow-pits at Berkner Island, with summer maxima in dust deposition, attributed to Southern South American sources, based on isotopic composition (Bory et al. 2010), in agreement with our simulation (Fig. 11c).

Previous modeling work showed summertime maxima in some dust studies (e.g. Genthon 1992; Lunt and Valdes 2002b), but idealized tracers show maxima in wintertime (Krinner et al. 2010), while transport efficiency was estimated to be maximum in winter (Lunt and Valdes 2001). Differences appear in coastal versus inland sites.

3.6 Variations in dust size

3.6.1 *Model results versus observations*

Mineral dust records from ice cores include size distribution, often described by either a lognormal (Royer et al. 1983) or a Weibull distribution (Delmonte et al. 2004a) with modal diameter around 1.5–2.0 μm (Royer et al. 1983). The small dimensions of the particles derive from deposition processes that are responsible for size fractionation during long range transport, increasing the fraction of small particles with increasing atmospheric residence time (Junge 1977; Tegen and Lacis 1996).

Variations in dust size with changing climate conditions have been observed, with shifts towards either finer or coarser dimensions in colder climates depending on the site (e.g. Ruth et al. 2003; Delmonte et al. 2004a). These size variations have been tentatively attributed to changes in the intensity and/or patterns of the atmospheric circulation in different climatic conditions (Junge 1977; Delmonte et al. 2004a), but other mechanisms such as deposition processes (Unnerstad and Hansson 2001) or size altering in-cloud processing (Wurzler et al. 2000) are likely involved and an attribution of the relative importance of all these aspects to determine the features shown by observations is still uncertain (Ruth et al. 2003; Fischer et al. 2007).

In Antarctica an opposite response to climatic changes of dust deposited at Vostok and Dome B (coarser in LGM) compared to EDC and Komsomolskaya (finer in LGM) was

Table 6 Dust size observations versus model (b2/b3)

Site—period	EDC—cur	EDC—LGM	EDC—LGM/cur	Talos—cur	Talos—LGM	Talos—LGM/cur	JRI—cur
Obs. (mean)	1.82	2.64	1.45	1.3	2.07	1.59	1.47
Obs. (SD)	0.52	0.53		0.33	0.57		
Model 1-year	0.97	1.23	1.27	1.25	1.66	1.33	1.39
Model 10-years (mean)	1.24	1.32	1.06	1.4	1.62	1.16	1.45
Model 10-years (SD)	0.1	0.14		0.11	0.19		0.11
Reference	Delmonte et al. (2004a)			Albani et al. (submitted)			McConnell et al. (2007)

observed (Delmonte et al. 2004a). The association of finer particles with cold climates and relatively coarse ones with warmer climates was shown to hold at EDC for eight glacial-interglacial cycles (Lambert et al. 2008). Preliminary results from EDML seem to indicate rather similar particle size during the Holocene and the LGM, but with individual coarse-particle events occurring mainly during the Holocene (Fischer et al. 2007).

In the present study the model includes dust in 4 size bins: bin1 = 0.1–1.0 μm; bin2 = 1.0–2.5 μm; bin3 = 2.5–5.0 μm; bin4 = 5.0–10.0 μm. In order to describe variations in dust size we use the bin2/bin3 (b2/b3) ratio as a metric, with high values of b2/b3 indicating abundance of fine particles. The choice is motivated to focus on the 1–5 μm range, similar to the observational range.

We performed a detailed comparison of modeled versus observed size distributions (Table 6), where data were available for exactly matching the model's size bins. The model is able to predict realistically the size distribution at JRI, and also reasonably well the size distributions in both current climate and the LGM at Talos Dome, but underestimates the fine fraction at EDC. The LGM/current ratios are captured in terms of the direction of change, but not fully in the magnitude. There are a number of possible causes explaining the difference with the observed size distributions at EDC, and for the underestimation of the magnitude of the observed LGM/current size shift. Here we list the potential ones that emerged from previous sections of this manuscript. They include: too much coarse particles emitted from the source areas, mismatched transport pathways (either due the geographic location of source areas or the seasonal cycle of dust mobilization), too weak removal of coarse particles en route, and/or too intense transport to inland Antarctica due to the coarse model grid flattening the edges of the plateau, with too short lifetimes and not enough time for larger particles to settle before they reach the interior of the plateau. Possible additional causes include the underestimation of high-tropospheric transport/subsidence from the stratosphere (e.g. Delmonte et al. 2004a; Krinner et al. 2010; Han and Zender 2010).

For a more extensive comparison with observations, we use the bin2/bin3 metric to compare with additional observations in a more qualitative way. The model simulates an increase in the fine particle fraction over most of the Southern Hemisphere in the LGM (Fig. 12a), that is consistent with observations at several sites (EDC: Lambert et al. 2008; Komsomolskaya: Delmonte et al. 2004a; EDML: Fischer et al. 2007; Talos Dome: Albani et al., submitted; Delmonte et al. 2010b), but contradicts with Dome B (Delmonte et al. 2004a). On the other hand a decrease in the fine particle fraction is modeled and observed at Vostok in the LGM (Delmonte et al. 2004a).

It is interesting to note that the model is able to capture an area in central Antarctica (and some areas in Western Antarctica) where the size of dust deposited during LGM increases. A possible explanation for the mismatch at one station (Dome B) can be related to the spatial resolution of the model and to biases in the modeled parameters controlling the dust cycle. We consider next the mechanisms in the model that produce these changes in dust size in the deposition.

3.6.2 Dust size changes: wet versus dry deposition

We analyze the physical causes of dust size variations in response to climatic changes in the climate model simulations, looking at changes in the (1) source areas, (2) transport patterns and (3) deposition mechanisms.

In the model used for this study, the relative fraction in each size bin of dust mobilization from every grid cell is kept fixed. In the real world, changes in source area and wind strength could have changed the size distribution of the source material (Alfaro and Gomes 2001), but these effects are not included in the model simulation. However, the model enables us to see that other mechanisms than source area or wind changes are able to produce the feature of different size changes in response to climate forcings. As already discussed in Sect. 3.2, the location and/or intensity of dust mobilization from the source areas has changed from the LGM to current climate. In particular the activity

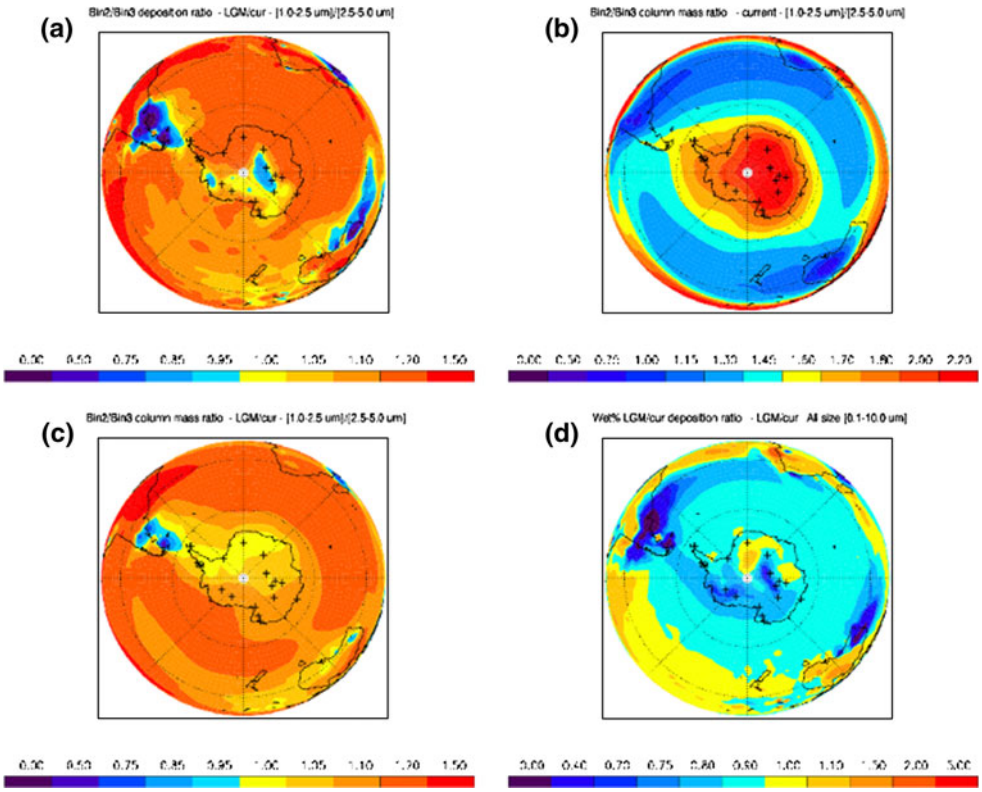

Fig. 12 Dust size variations from model simulation. The bin2/bin3 ratio for either dust deposition flux or column dust loading is chosen as as size parameter. High values for bin2/bin3 indicate relative abundance of fine particles. **a** LGM/current climate ratio for the bin2/bin3 size parameter (deposition flux). **b** bin2/bin3 (column loading) size parameter for current climate. **c** LGM/current climate ratio for the bin2/bin3 size parameter (column loading). **d** LGM/current climate ratio for the wet deposition fraction (wet%), expressed as a percentage of total (wet + dry) dust deposition

of glaciogenic sources in Southern SAM markedly decreased since the LGM.

We now analyze size fractionation during transport, as simulated in the model. The 10-year simulation for the current climate (Fig. 12b) clearly shows the effects of size selection during long-range transport, leading to a net shift towards finer dimensions with increasing latitudes for dust suspended into the atmosphere (Junge 1977), in agreement with other work (Tegen and Lacis 1996). The LGM/current ratio from the model (Fig. 12c) shows that, with the only exception of limited areas downwind of the glacial Patagonian sources, there is everywhere an increase of fine particles. This is consistent with a reduction in wet deposition and a lengthening of dust lifetimes over the Southern Ocean, since fine particles are preferentially removed by wet deposition (Fig. 8).

Size-resolved dust loading vertical profiles for current climate and for the LGM are compared, with a typical bimodal distribution of dust loading in function of height simulated for current climate (Fig. 13, upper panel and Fig. 5), contrasting with an overall roughly mono-modal distribution in the LGM (Fig. 13, bottom panel). In particular, for current climate (Fig. 13, upper panel) small particles (bin1 and bin2) profiles show a double peak, in phase at bottom levels and slightly shifted in the upper ones. Large particles (bin3 and bin4) instead show mono-modal distributions, in phase with the small particles' lower peak. These features may suggest a more direct mid-tropospheric transport corresponding to the lower peak shared by all size classes and an upper peak close to the tropopause characteristic of long-lived small dust particles (see Fig. 6 for meridional averages).

On the other hand LGM size-resolved dust loading vertical profiles (Fig. 13, bottom panel) have an overall roughly mono-modal distribution, as discussed in Sect. 3.3.2. The peaks at higher levels for smaller particles are more evident in winter (JJA), when the dust loading is at minimum. The picture is roughly the same for SAM dust and for other sites (Talos Dome and EPICA Dronning Maud Land, not shown) and for zonal averages (Fig. 6). The vanishing of the double-peak in the LGM profiles, is preferentially a loss for the small particles, which then remain closer to the surface, and suffer more loss through deposition (see also Sect. 3.4.1).

The model slightly overestimates wet deposition generally speaking (Mahowald et al. 2011), and problems with accumulation discussed in Sect. 3.1 may contribute to this in Antarctica. For coastal sites in Antarctica the simulated relative contribution of wet dust deposition to the total deposition is ~90%, which matches the observational based estimates (Wolff et al. 1998). On the other hand, in the interior of Antarctica the simulated wet deposition accounts for at least 60% of total dust deposition, while observational estimates suggest that dry deposition dominates there (Legrand and Mayewski 1997). In particular it is estimated that dry deposition accounts for 75% of the

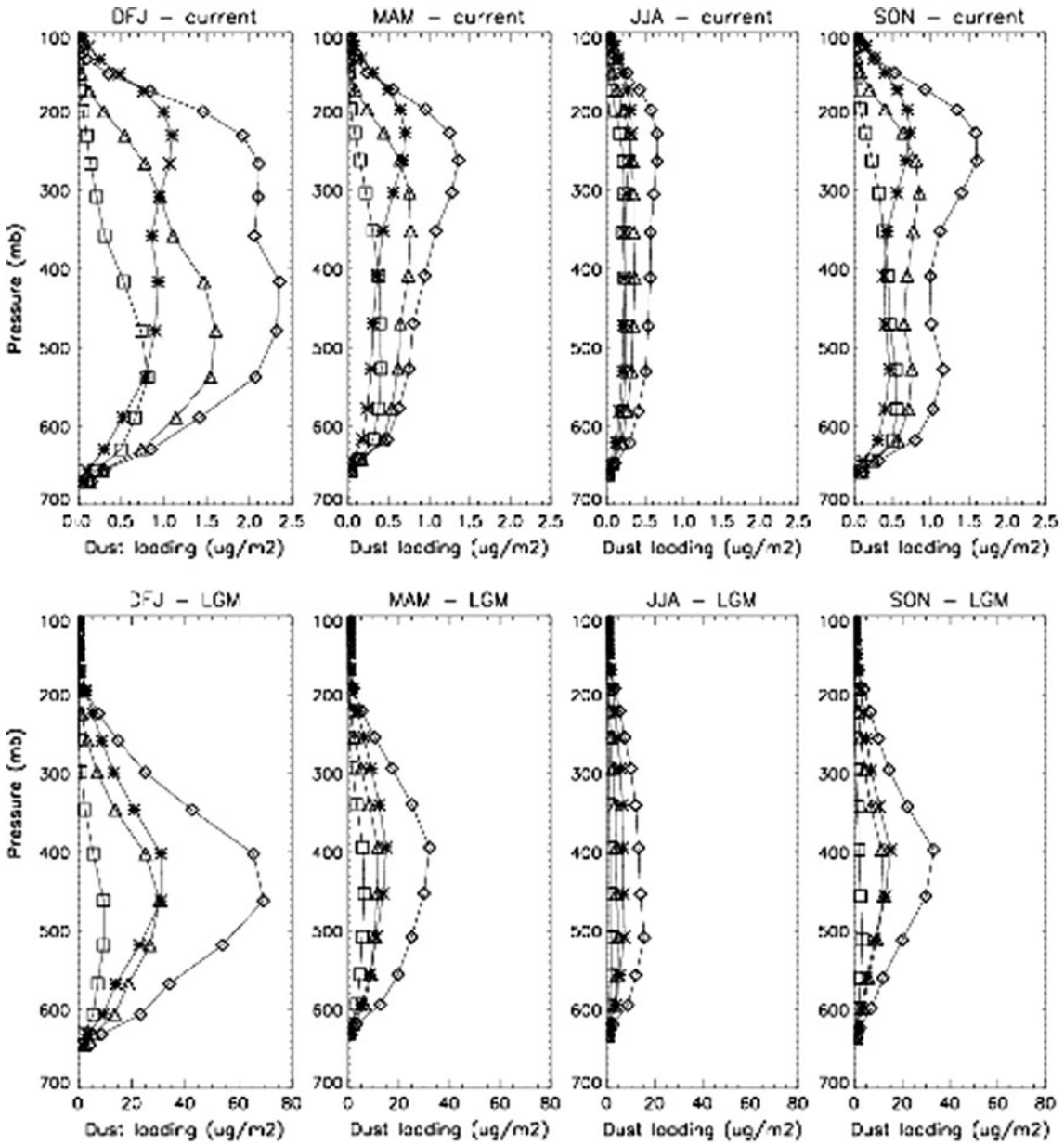

Fig. 13 Seasonal evolution of size-resolved vertical profiles of AUS dust loading over Dome C, simulated for the current (*top*) and LGM (*bottom*) climate. From left to right plots for the different seasons: summer (DJF), autumn (MAM), winter (JJA) and spring (SON). Stars: bin1 (0.1–1.0 μm). *Diamonds*: bin2 (1.0–2.5 μm). *Triangles*: bin3 (2.5–5.0 μm). *Squares*: bin4 (5.0–10.0 μm)

total aerosol deposition at EDML (Göktas et al. 2002) and 80% at EDC (Wolff et al. 2006). Note that there are no direct observations of dust deposition mechanisms for Antarctica, because of difficulties related to the very low concentrations and deposition rates (Bigler et al. 2006), so the estimates are based on other aerosol species deposition mechanisms (Wolff et al. 1998; Legrand and Mayewski 1997; Wolff et al. 2006).

Variations in dust deposition mechanisms in the model are summarized using the LGM/current climate ratio for the wet deposition fraction over total dust deposition (Fig. 12d). The resemblance of its spatial features with those of the size parameter (Fig. 12a), suggests a possible clue for explaining dust size variations, given the size-selective nature of dry deposition (Unnerstad and Hansson 2001). Observational and model based estimates suggest a halving of snow accumulation during the LGM on the East Antarctic Plateau (e.g. EPICA Community Members 2006). While previous studies have suggested that the fraction of the time where there is precipitation is more important than the amount of precipitation for wet deposition removal (Mahowald et al. 2011), it is likely that this lowering of precipitation is associated with an increased importance of dry deposition compared to wet deposition.

Table 7 Average Antarctic (as defined for Fig. 14) Pearson's correlation coefficient calculated for time series at monthly resolution of the b2/b3 metric and the wet% metric, for different simulations and climate period

Simulation	Current climate	LGM climate
10-years base (120 months)	0.753	0.720
1-year total (12 months)	0.823	0.754
1-year SAM (12 months)	0.820	0.724
1-year AUS (12 months)	0.545	0.710

There is a strong temporal (Table 7) and spatial (Fig. 14) correlation between the change in the size fraction (b2/b3 ratio LGM/cur) and the fraction of dust wet deposited (wet% LGM/cur). This is independent of which set of model simulations we use, or which sources are analyzed (Fig. 14). This suggests that the relative importance of wet deposition plays a role. In regions with very low dust deposition, and snow accumulation (Fig. 14), there tends to be a low value of the b2/b3 LGM/current ratio (Fig. 14).

The size fractionation of dust deposited over Antarctica represents the end-term of a complex process. As such, all the uncertainties and biases in the model discussed throughout the text, including uncertainties in dust deposition fluxes and/or snow deposition discussed in Sect. 3.1, may contribute to a large uncertainty in some of our results.

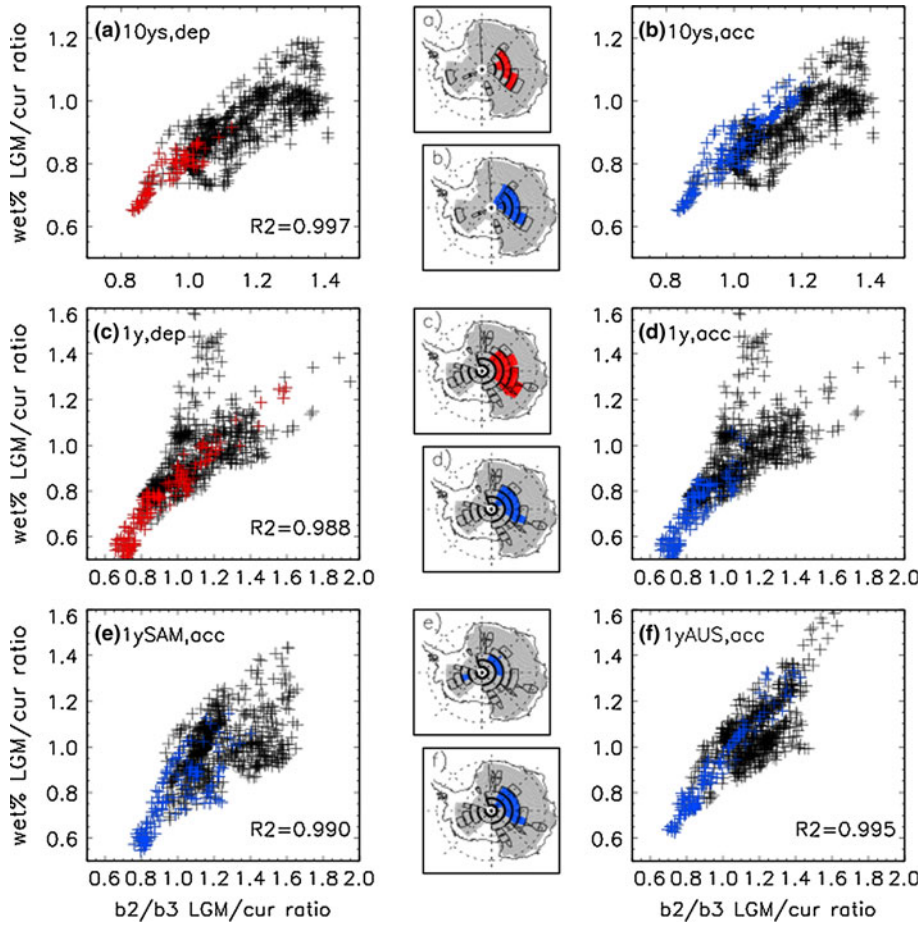

Fig. 14 Scatterplots for the b2/b3 LGM/cur versus wet% LGM/cur metrics from the model simulations. The b2/b3 LGM/cur metric is the LGM/current ratio of bin2/bin3 in dust deposition, which represents the shift toward finer modes in dust size distributions in the LGM (so b2/b3 LGM/cur <1 represents an increase in particles' size, like observations at Vostok). The wet% LGM/cur metric is the LGM/current ratio in the proportion (fraction) of wet deposition of dust, that represents the tendency to increase of the proportion of wet deposition compared to dry deposition of dust in the LGM, compared to current climate (in this case wet% LGM/cur <1 represents a decrease in the relative importance of wet deposition in the LGM, that corresponds to an increase in the relative proportion of dry deposition to the dust deposition budget). Points in the scatterplots represent Antarctica, defined arbitrarily as the model grid cells at latitudes <65°S and elevation >500 m a.s.l., and represented by *grey shading* on the maps in the central column. *Black lines* shading on the maps in the central column correspond to point with b2/b3 LGM/cur <1. Superimposed on scatterplots and corresponding maps are points with LGM absolute values of either dust deposition (*red colors*) or snow accumulation (*blue colors*) below a fixed threshold—10 mg m^{-2} $year^{-1}$ for dust deposition and 12 cm w.e./year for snow accumulation. Values of R^2 for the scatterplots are also reported

4 Conclusions

The focus of this work is the variations in dust deposition fluxes, grain size and provenance in simulations of the current and the Last Glacial Maximum climates, compared with available data. The model provides a self-consistent framework for explaining the changes in deposition and deposited particles, although the model results may be in error.

We compare simulated deposition rates and dust concentrations in ice cores with observations, including most recent available data. As previously shown (Mahowald et al. 2006) the model is able to capture the magnitude order of those parameters, for both LGM and current climate, though capturing the spatial distribution of the LGM/current ratio in dust deposition tends to be difficult, even after tuning the source activity. The case-to-case differences are of diverse amplitude and may be attributed to biases and uncertainties in models and observations, and to some extent are also inherent in the comparison itself.

Transport patterns from the Southern Hemisphere dust source areas usually follow zonal patterns, while meridional transport is controlled by eddies (Li et al. 2010a). We suggest here that access points to Antarctica are located in specific areas characterized by southward displacement of air masses (Parish and Bromwich 2007), with subsequent mixing and redistribution of dust within the Antarctic atmospheric circulation. This process appears controlled by the Antarctic atmospheric circulation, and it is characterized by an annual seasonal cycle showing austral summer maxima for meridional dust transport.

In some locations in the Southern Ocean and Antarctic, there are large increases in deposition between the LGM and current climate, and this is quite spatially diverse in relation to specific source areas. The increase in source strength is not expected to be the same as the increase in deposition seen everywhere downwind since the atmosphere is 3-dimensional, and sources and transport pathways can vary with climate change. In particular, after examining the possible mechanisms responsible for the large ratios in deposition observed in the Antarctic ice cores (e.g. Petit et al. 1999; Lambert et al. 2008), we suggest, based on the model's output, that multiple processes likely act together, through an amplification chain that finally leads to a magnification of glacial/interglacial concentration ratio: increased activity of the source areas, more efficient transport, reduced en route removal and easier deposition over Antarctica because of the lower levels of transport. This latter mechanism in particular is related to the preferential concentration of airborne dust in the lower levels of the troposphere above Antarctica.

Finally, we show for the first time a comparison between model results and the observed spatial variability of dust size response to climate variations (Delmonte et al. 2004a). The model is able to reproduce the increased grain size in the LGM in some areas over central Eas Antarctica, opposed to a generalized shift toward finer particle in the Southern Hemisphere and over most Antarctica in particular. We analyze the possible mechanisms that could explain this feature, and suggest that the generalized increase in the fine fraction in the LGM was probably related to the reduced en route wet removal. On the other hand, a key role is also played by the relative proportion of dry and wet deposition, an enhanced relative contribution of dry deposition (size-selective) leading to increased particles size in some areas.

Acknowledgments N. M. Mahowald and S. Albani acknowledge the support of NSF-0832782, NSF-0745961, NSF-0932946, NSF-1003509 and NASA-NNG06G127G. The computer simulations used in this study were performed at the National Center for Atmospheric Research, a National Science Foundation facility. S. Albani acknowledges funding from "Dote ricercatori": FSE, Regione Lombardia. We gratefully acknowledge Joseph Prospero for providing us with dust surface concentration data from in situ measurements from the University of Miami Ocean Aerosol Network. We would also like to thank two anonymous reviewers for their constructive comments that helped improving the manuscript.

References

Albani S, Delmonte B, Maggi V, Baroni C, Petit JR, Stenni B, Mazzola C, Frezzotti M (submitted) Last glacial to Holocene large-scale and regional atmospheric and dust changes at Talos Dome, East Antarctica. Geophys Res Lett

Alfaro SC, Gomes L (2001) Modeling mineral aerosol production by wind erosion: emission intensities and aerosol size distributions in source areas. J Geophys Res 106(D16):18,075–18,084

Andersen KK, Ditlevsen PD (1998) Glacial/interglacial variations of meridional transport and washout of dust: a one-dimensional model. J Geophys Res 103(D8):8955–8962

Andersen KK, Armengaud A, Genthon C (1998) Atmospheric dust under glacial and interglacial conditions. Geophys Res Lett 25(13):2281–2284

Basile I, Grousset FE, Revel M, Petit J-R, Biscaye PE, Barkov NI (1997) Patagonian origin of glacial dust deposited in East Antarctica (Vostok and Dome C) during glacial stages 2, 4 and 6. Earth Planet Sci Lett 146:573–589

Bigler M, Rothlisberger R, Lambert F, Stocker TF, Wagenbach D (2006) Aerosol deposited in East Antarctica over the last glacial cycle: detailed apportionment of continental and sea-salt contributions. J Geophys Res 111:D08205. doi:10.1029/2005JD006469

Bory AE, Wolff E, Mulvaney R, Jagoutz E, Wegner A, Ruth U, Elderfield H (2010) Multiple sources supply eolian mineral dust to the Atlantic sector of coastal Antarctica: evidence from recent snow layers at the top of Berkner Island ice sheet. Earth Planet Sci Lett 291:138–148. doi:10.1016/j.epsl.2010.01.006

Burn-Nunes LJ, Vallelonga P, Loss RD, Burton GR, Moy A, Curran M, Hong S, Smith AM, Edwards R, Morgan VI, Rosman KJR (2011) Seasonal variability in the input of lead, barium and indium to Law Dome, Antarctica. Geochimica et Cosmochimica Acta 75:1–20

Collins WD, Bitz CM, Blackmon ML, Bonan GB, Bretherton CS, Carton JA, Chang P, Doney SC, Hack JJ, Henderson TB, Kiehl

JT, Large WG, McKenna DS, Santer BD, Smith RD (2006) The community climate system model version 3 (CCSM3). J Climate 19(11):2122–2143

Cunningham WC, Zoller WH (1981) The chemical composition of remote area aersols. J Aerosol Sci 12(4):367–384

Delaygue G, Masson V, Jouzel J, Koster RD, Healy RJ (2000) The origin of Antarctic precipitation: a modelling approach. Tellus B 52:19–36

Delmonte B, Petit JR, Maggi V (2002) Glacial to Holocene implications of the new 27000-year dust record from the EPICA Dome C (East Antarctica) ice core. Clim Dyn 18:647–660. doi:10.1007/s00382-001-0193-9

Delmonte B, Petit J-R, Andersen KK, Basile-Doelsch I, Maggi V, Lipenkov VY (2004a) Dust size evidence for opposite regional atmospheric circulation changes over east Antarctica during the last climatic transition. Clim Dyn 23:427–438. doi:10.1007/s00382-004-0450-9

Delmonte B, Basile-Doelsch I, Petit J-R, Maggi V, Revel-Rolland M, Michard A, Jagoutz E, Grousset F (2004b) Comparing the Epica and Vostok dust records during the last 220,000 years: stratigraphical correlation and provenance in glacial periods. Earth-Sci Rev 66:63–87

Delmonte B, Petit J-R, Basile-Doelsch I, Jagoutz E, Maggi V (2007) Late Quaternary Interglacials in East Antarctica From Ice-Core Dust Records. In: Sirocko F, Litt T, Clausen M (eds) The climate of past interglacials. Elsevier, Amsterdam, pp 53–73

Delmonte B, Delmas RJ, Petit J-R (2008a) Comment on ''Dust provenance in Antarctic ice during glacial periods: from where in southern South America?'' by D. M. Gaiero. Geophys Res Lett 35:L08707. doi:10.1029/2007GL032075

Delmonte B, Andersson PS, Hansson M, Schöberg H, Petit J-R, Basile-Doelsch I, Maggi V (2008b) Aeolian dust in East Antarctica (EPICA-Dome C and Vostok): provenance during glacial ages over the last 800 kyr. Geophys Res Lett 35:L07703. doi:10.1029/2008GL033382

Delmonte B, Andersson PS, Schöberg H, Hansson M, Petit J-R, Delmas R, Gaiero DM, Maggi V, Frezzotti M (2010a) Geographic provenance of aeolian dust in East Antarctica during Pleistocene glaciations: preliminary results from Talos Dome and comparison with East Antarctic and new Andean ice core data. Quat Sci Rev. doi:10.1016/j.quascirev.2009.05.010

Delmonte B, Baroni C, Andersson PS, Schoberg H, Hansson M, Aciego S, Petit J-R, Albani S, Mazzola C, Maggi V, Frezzotti M (2010b) Aeolian dust in the Talos Dome ice core (East Antarctica, Pacific/Ross Sea sector): Victoria Land versus remote sources over the last two climate cycles. J Quat Sci. doi:10.1002/jqs.1418

Dentener F, Carmichael G, Zhang Y, Lelieveld J, Crutzen P (1996) Role of mineral aerosol as a reactive surface in the global troposphere. J Geophys Res 101(D17):22869–22889

Dickerson RR, Kondragunta S, Stenchikov G, Civerolo KL, Doddridge BG, Holben BN (1997) The impact of aerosols on solar ultraviolet radiation and photochemical smog. Science. doi:10.1126/science.278.5339.827

EPICA community members (2004) Eight glacial cycles from an Antarctic ice core. Nature, VOL 429, 10 JUNE 2004

EPICA Community Members (2006) One-to-one coupling of glacial climate variability in Greenland and Antarctica. Nature 444:195–198. doi:10.1038/nature05301

Fischer H, Siggaard-Andersen ML, Ruth U, Rothlisberger R, Wolff E (2007) Glacial/interglacial changes in mineral dust and sea-salt records in polar ice cores: sources, transport, and deposition. Rev Geophys 45:RG1002. doi:10.1029/2005RG000192

Frezzotti M, Urbini S, Proposito M, Scarchilli C, Gandolfi S (2007) Spatial and temporal variability of surface mass balance near Talos Dome, East Antarctica. J Geophys Res 112:F02032. doi:10.1029/2006JF000638

Gabrielli P, Wegner A, Petit J-R, Delmonte B, DeDeckker P, Gaspari V, Fisher H, Ruth U, Kriews M, Boutron C, Cescon P, Barbante C (2010) A major glacial-interglacial change in aeolian dust composition inferred from Rare Earth Elelments in Antarctica ice. Quat Sci Rev. doi:10.1016/j.quascirev.2009.09.002

Gaiero DM (2008) Reply to comment by B. Delmonte et al. on "Dust provenance in Antarctic ice during glacial periods: from where in southern South America?" Geophys Res Lett 35:L08708. doi:10.1029/2007GL032477

Gaiero DM, Probst J-L, Depetris PJ, Bidart SM, Leleyter L (2003) Iron and other transition metals in Patagonian riverborne and windborne materials: geochemical control and transport to the southern South Atlantic Ocean. Geochimica et Cosmochimica Acta 67(19):3603–3623. doi:10.1016/S0016-7037(03)00211-4

Gaiero DM, Brunet F, Probst J-L, Depretis PJ (2007) A uniform isotopic and chemical signature of dust exported from Patagonia: rock sources and occurrence in southern environments. Chem Geol 238(1–2):107–120

Gassó S, Stein AF (2007) Does dust from Patagonia reach the sub-Antarctic Atlantic Ocean? Geophys Res Lett 34:L01801. doi:10.1029/2006GL027693

Gassó S, Stein A, Marino F, Castellano E, Udisti R, Ceratto J (2010) A combined observational and modeling approach to study modern dust transport from the Patagonia desert to East Antartica. Atmos Chem Phys 10:8287–8303. doi:10.5194/acp-10-8287-2010

Genthon C (1992) Simulations of desert dust and sea-salt aerosols in Antarctica with a general circulation model of the atmosphere. Tellus 44B:371–389

Ginoux P, Chin M, Tegen I, Prospero J, Holben B, Dubovik O, Lin S-J (2001) Sources and distributions of dust aerosols simulated with the GOCART model. J Geophys Res 106(D17):20255–20273

Göktas F, Fischer H, Oerter H, Weller R, Sommer S, Miller H (2002) A glacio-chemical characterization of the new EPICA deep-drilling site on Amundsenien, Dronning Maud Land, Antarctica. Ann Glaciol 35:347–354

Grousset FE, Biscaye PE (2005) Tracing dust sources and transport patterns using Sr, Nd and Pb isotopes. Chem Geol 222:149–167

Grousset FE, Biscaye PE, Revel M, Petit J-R, Pye K, Joussaume S, Jouzel J (1992) Antarctic (Dome C) ice-core dust at 18 k.y.B.P.: Isotopic constraints on origins. Earth Planet Sci Lett 111:175–182

Han Q, Zender CS (2010) Desert dust aerosol age characterized by mass-age tracking of tracers. J Geophys Res 115:D22201. doi:10.1029/2010JD014155

Haxeltine A, Prentice IC (1996) BIOME3: an equilibrium terrestrial biosphere model based on ecophysiological constraints, resource availability, and competition among plant functional types. Global Biogeochem Cycles 10(4):693–709

Holben BN, Eck TF, Slutsker I, Tanré D, Buis JP, Setzer A, Vermote E, Reagan JA, Kaufman YJ, Nakajima T, Lavenu F, Jankowiak I, Smirnov A (1998) AERONET: a federated instrument network and data archive for aerosol characterization. Remote Sens Env 66:1–16

Hou SG, Li YS, Xiao CD, Ren JW (2007) Recent accumulation rate at Dome Argus, Antarctica. Chinese Sci Bull J 52(3):428–431

Jickells TD, An ZS, Andersen KK, Baker AR, Bergametti G, Brooks N, Cao JJ, Boyd PW, Duce RA, Hunter KA, Kawahata H, Kubilay N, LaRoche J, Liss PS, Mahowald NM, Prospero JM, Ridgwell AJ, Tegen I, Torres R (2005) Global iron connections between desert dust, ocean biogeochemistry, and climate. Science 308:67. doi:10.1126/science.1105959

Johnson MS, Meskhidze N, Solmon F, Gassó S, Chuang PY, Gaiero DM, Yantosca RM, Wu S, Wang Y, Carouge C (2010) Modeling dust and soluble iron deposition to the South Atlantic Ocean. J Geophys Res 115:D15202. doi: 10.1029/2009JD013311

Joussaume S (1990) Three-dimensional simulations of the atmospheric cycle of desert dust particles using a general circulation model. J Geophys Res 95(D2):1909–1941

Joussaume S (1993) Paleoclimatic tracers: an investigation using an atmospheric general circulation model under ice age conditions 1. Desert Dust J Geophys Res 98(D2):2767–2805

Junge CE (1977) Processes responsible for the trace content in precipitation. In: Isotopes and impurities in ice and snow, IAHS-AISH Publ. 118, Int Assoc Hydrol Sci Grenoble

Kameda T, Motoyama H, Fujita S, Takahashi S (2008) Temporal and spatial variability of surface mass balance at Dome Fuji, East Antarctica, by the stake method from 1995 to 2006. J Glaciol 54(184):107–116

Kaufman YJ, Tanré D, Boucher O (2002) A satellite view of aerosols in the climate system. Nature 419:215–223

Kiehl JT, Shields CA, Hack JJ, Collins WD (2006) The climate sensitivity of the community climate system model version 3 (CCSM3). J Clim 19(11):2584–2596

King JC, Turner J (1997) Antarctic meteorology and climatology. In: Dessler AJ, Houghton JT, Rycroft MJ (eds) Cambridge atmospheric and space science series. Cambridge University Press, Cambridge

Kohfeld KE, Harrison SP (2001) DIRTMAP: the geological record of dust. Earth Sci Rev 54:81–114

Krinner G, Genthon C (1998) GCM simulations of the Last Glacial Maximum surface climate of Greenland and Antarctica. Clim Dyn 14(10):741–758

Krinner G, Genthon C (2003) Tropospheric transport of continental tracers towards Antarctica under varying climatic conditions. Tellus 55B:54–70

Krinner G, Petit J-R, Delmonte B (2010) Altitude of atmospheric tracer transport towards Antarctica in present and glacial climate. Quat Sci Rev. doi:10.1016/j.quascirev.2009.06.020

Lambert F, Delmonte B, Petit J-R, Bigler M, Kaufmann PR, Hutterli MA, Stocker TF, Ruth U, Steffensen JP, Maggi V (2008). Dust-climate couplings over the past 800,000 years from the EPICA Dome C ice core. Nature 452. doi:10.1038/nature06763

Lanci L, Delmonte B, Maggi V, Petit J-R, Kent DV (2008) Ice magnetization in the EPICA-Dome C ice core: implication for dust sources during glacial and interglacial periods. J Geophys Res 113:D14207. doi:10.1029/2007JD009678

Legrand M, Mayewski P (1997) Glaciochemistry of polar ice cores: a review. Rev Geophys 35(3):219–243

Levin Z, Ganor E, Gladstein V (1996) The effects of desert particles coated with sulfate on rain formation in the eastern Mediterranean. J Appl Met 35(9):1511–1523

Li F, Ginoux P, Ramaswamy V (2008) Distribution, transport, and deposition of mineral dust in the Southern Ocean and Antarctica: Contribution of major sources. J Geophys Res 113:D10207. doi: 10.1029/2007JD009190

Li F, Ginoux P, Ramaswamy V (2010a) Transport of patagonian dust to Antarctica. J Geophys Res 115:D18217. doi:10.1029/2009JD012356

Li F, Ramaswamy V, Ginoux P, Broccoli AJ, Delworth T, Zeng F (2010b) Toward understanding the dust deposition in Antarctica during the Last Glacial Maximum: sensitivity studies on plausible causes. J Geophys Res 115:D24120. doi:10.1029/2010JD014791

Lunt DJ, Valdes PJ (2001) Dust transport to Dome C, Antarctica, at the Last Glacial Maximum and present day. Geophys Res Lett 28(2):295–298

Lunt DJ, Valdes PJ (2002a) Dust deposition and provenance at the Last Glacial Maximum and present day. Geophys Res Lett. doi: 10.1029/2002GL015656

Lunt DJ, Valdes PJ (2002b) The modern dust cycle: comparison of model results with observations and study of sensitivities. J Geophys Res 107:D23. doi:10.1029/2002JD002316

Mahowald NM (2007) Anthropocene changes in desert area: Sensitivity to climate model predictions. Geophys Res Lett 34:L18817. doi:10.1029/2007GL030472

Mahowald NM, et al (2008) Global distribution of atmospheric phosphorus sources, concentrations and deposition rates, and anthropogenic impacts. Global Biogeochem Cycles 22:GB4026. doi:10.1029/2008GB003240

Mahowald N, Kohfeld K, Hansson M, Balkanski Y, Harrison SP, Prentice IC, Schulz M, Rodhe H (1999) Dust sources and deposition during the Last Glacial Maximum and current climate: a comparison of model results with paleodata from ice cores and marine sediments. J Geophys Res 104(D13):15895–15916

Mahowald NM, Muhs DR, Levis S, Rasch PJ, Yoshioka M, Zender CS, Luo C (2006) Change in atmospheric mineral aerosols in response to climate: last glacial period, preindustrial, modern, and doubled carbon dioxide climates. J Geophys Res 111: D10202

Mahowald NM, Engelstaedter S, Luo C, Sealy A, Artaxo P, Benitez-Nelson C, Bonnet S, Chen Y, Chuang PY, Cohen DD, Dulac F, Herut B, Johansen AM, Kubilay N, Losno R, Maenhaut W, Paytan A, Prospero JM, Shank LM, Siefert RL (2009) Atmospheric iron deposition: global distribution, variability, and human perturbations. Ann Rev Mar Sci 1:245–278. doi:10.1146/annurev.marine.010908.163727

Mahowald NM, Albani S, Engelstaedter S, Winckler G, Goman M (2011) Model insight into paleodust records. Quat Sci Rev 30(7–8):832–854

Marino F, Castellano E, Ceccato D, De Deckker P, Delmonte B, Ghermanti G, Maggi V, Petit J-R, Revel-Rolland M, Udisti R (2008) Defining the geochemical composition of the EPICA Dome C ice core dust during the last glacial-interglacial cycle. Geochem Geophys Geosyst 9:Q10018. doi:10.1029/2008GC002023

Marino F, Castellano E, Nava S, Chiari M, Ruth U, Wegner A, Lucarelli F, Udisti R, Delmonte B, Maggi V (2009) Coherent composition of glacial dust on opposite sides of the East Antarctic Plateau inferred from the deep EPICA ice cores. Geophys Res Lett 36:L23703. doi:10.1029/2009GL040732

Martin JH, Gordon RM, Fitzwater SE (1990) Iron in Antarctic waters. Nature 353(6340):123

Martínez-García A, Rosell-Melé A, Geibert W, Gersonde R, Masqué P, Gaspari V, Barbante C (2009) Links between iron supply, marine productivity, sea surface temperature, and CO_2 over the last 1.1 Ma. Paleoceanography 24:PA1207. doi:10.1029/2008PA001657

Masson-Delmotte V, Stenni B, Pol K, Braconnot P, Cattani O, Falourd S, Kageyama M, Jouzel J, Landais A, Minster B, Barnola JM, Chappellaz J, Krinner G, Johnsen S, Röthlisberger R, Hansen J, Mikolajewicz U, Otto-Bliesner B (2010) EPICA Dome C record of glacial and interglacial intensities. Quat Sci Rev 29:113–128. doi:10.1016/j.quascirev.2009.09.030

McConnell JR, Aristarain AJ, Banta JR, Edwards PR, Simoes JC (2007) 20th-Century doubling in dust archived in an Antarctic Peninsula ice core parallels climate change and desertification in South America. PNAS 104(14):5743–5748

McTainsh GH, Lynch AW (1996) Quantitative estimates of the effect of climate change on dust storm activity in Australia during the Last Glacial Maximum. Geomorphology 17:263–271

Miller RL, Tegen I (1998) Climate response to soil dust aerosols. J Clim 11(12):3247–3267

Mumford JW, Peel DA (1982) Microparticles, marine salts and stable isotopes in a shallow firn core from the Antarctic Peninsula. Br Antarct Surv Bull 56:37–47

Noone D, Simmonds I (2002) Annular variations in moisture transport mechanisms and the abundance of $\delta^{18}O$ in Antarctic snow. J Geophys Res 107:D24. doi:10.1029/2002JD002262

Otto-Bliesner BE, Brady EC, Clauzet G, Tomas R, Levis S, Kothavala Z (2006) Last Glacial Maximum and holocene climate in CCSM3. J Clim 19:2526–2544

Parish TR, Bromwich DH (2007) Reexamination of the near-surface airflow over the antarctic continent and implications on atmospheric circulations at high southern latitudes. Mon Weather Rev 135(5):1961–1973. doi: 10.1175/MWR3374.1

Penner JE et al (2001) Aerosols, their direct and indirect effect. In: Houghton JT et al (eds) Climate change 2001: the scientific basis. Cambridge University Press, New York

Petit J-R, Jouzel J, Raynaud D, Barkov NI, Barnola JM, Basile I, Bender M, Chappellaz J, Davisk M, Delaygue G, Delmotte M, Kotlyakov VM, Legrand M, Lipenkov VY, Lorius C, Pepin L, Ritz C, saltzmank E, Stievenard M (1999) Climate and atmospheric history of the past 420,000 years from the Vostok ice core, Antarctica. Nature 399(3):429–436

Petit JR, Delmonte B (2009) A model for large glacial–interglacial climate-induced changes in dust and sea salt concentrations in deep ice cores (central Antarctica): palaeoclimatic implications and prospects for refining ice core chronologies. Tellus B 61:768–790. doi: 10.1111/j.1600-0889.2009.00437.x

Prospero JM, Lamb PJ (2003) African droughts and dust transport to the caribbean: climate change implications. Science 302(5647): 1024–1027. doi: 10.1126/science.1089915

Prospero JM, Ginoux P, Torres O, Nicholson SE, Gill TE (2002) Environmental characterization of global sources of atmospheric soil dust identified with the Nimbus 7 Total Ozone mapping spectrometer (TOMS) Absorbing Aerosol Product Rev Geophys 40(1):1002. doi:10.1029/2000RG000095

Revel-Rolland M, De Deckker P, Delmonte P, Hesse PP, Magee JW, Basile-Doelsch I, Grousset F, Bosch D (2006) Eastern Australia: a possible source of dust in East Antarctica interglacial ice. Earth Planet Sci Lett 249:1–13

Rojas M, Moreno P, Kageyama M, Crucifix M, Hewitt C, Abe-Ouchi A, Ohgaito R, Brady EC, Hope P (2009) The Southern Westerlies during the Last Glacial Maximum in PMIP2 simulations. Clim Dyn 32:525–548. doi:10.1007/s00382-008-0421-7

Rosenfeld D, Rudich Y, Lahav R (2001) Desert dust suppressing precipitation: a possible desertification feedback loop. PNAS 98(11):5975–5980

Royer A, De Angelis M, Petit J-R (1983) A 30000 year record of physical and optical properties of microparticles from an east antarctic ice core and implications for paleoclimate reconstruction models. Climatic Change 5:381–412

Ruth U, Wagenbach D, Steffensen JP, Bigler M (2003) Continuous record of microparticle concentration and size distribution in the central Greenland NGRIP ice core during the last glacial period. J Geophys Res 108:D3. doi:10.1029/2002JD002376

Ruth U, Barbante C, Bigler M, Delmonte B, Fischer H, Gabrielli P, Gaspari V, Kaufmann P, Lambert F, Maggi V, Marino F, Petit J-R, Udisti R, Wagenbach D, Wegner A, Wolff EW (2008) Proxies and Measurement Techniques for Mineral Dust in Antarctic Ice Cores. Environ Sci Technol 42 (15): 5675–5681, doi: 10.1021/es703078z

Siggaard-Andersen M-L, Gabrielli P, Steffensen JP, Strømfeldt T, Barbante C, Boutron C, Fischer H, Miller H (2007) Soluble and insoluble lithium dust in the EPICA DomeC ice core–implications for changes of the East Antarctic dust provenance during the recent glacial–interglacial transition. Earth Planet Sci Lett 258:32–43

Smirnov A, Holben BN, Savoie D, Prospero JM, Kaufman YJ, Tanré D, Eck TF, Slutsker I (2000) Relationship between column aerosol optical thickness and in situ ground based dust concentrations over Barbados. Geophys Res Lett 27:1643–1646

Sokolik IN, Winker DM, Bergametti G, Gillette DA, Carmichael G, Kaufman YJ, Gomes L, Schuetz L, Penner JE (2001) Introduction to special section: outstanding problems in quantifying the radiative impacts of mineral dust. J Geophys Res 106:18015–18027

Sommer S, Wagenbach D, Mulvaney R, Fischer H (2000) Glaciochemical study spanning the past 2 kyr on three ice cores from Dronning Maud Land, Antarctica 2. Seasonally resolved chemical records. J Geophys Res 105(D24):29423–29433

Sugden DE, McCulloch RD, Bory AJM, Hein AS (2009) Influence of Patagonian glaciers on Antarctic dust deposition during the last glacial period. Nature Geosci 2. doi:10.1038/NGEO474

Tanaka TY, Chiba M (2006) A numerical study of the contributions of dust source regions to the global dust budget. Global Planet Change 52:88–104

Tegen I (2003) Modeling the mineral dust aerosol cycle in the climate system. Quat Sci Rev 22:1821–1834

Tegen I, Fung I (1994) *M*odeling of mineral dust in the atmosphere–sources, transport, and optical-thickness. J Geophys Res 99(D11): 22897–22914

Tegen I, Lacis AA (1996) Modeling of particle size distribution and its influence on the radiative properties of mineral dust aerosol. J Geophys Res 101(D14):19237–19244

Thompson LG (1975) Variations in microparticle concentration, size distribution and elemental composition found in Camp Century, Greenland, and Byrd station, Antarctica, deep ice cores. In: Isotopes and Impurities in Snow and Ice (Proceedings of a symposium held during the XVI Assembly of the International Union of Geodesy and Geophysics at Grenoble, August–September 1975). IAHS Publ. no. 118

Thompson LG (1977) Microparticles, ice sheets and climate. Reports of the Institute of Polar Studies, Ohio State University, No. 64, 148 pp

Thompson LG, Mosley-Thompson E, Petit JR (1981) Glaciological interpretation of microparticle concentrations from the French 905-m Dome C, Antarctica core. In: Sea Level, Ice, and Climatic Change (Proceedings of the Canberra Symposium, December 1979). IAHS Publ. no. 131

Thompson LG, Mosley-Thompson E, Davis ME, Lin PN, Henderson KA, Cole-Dai J, Bolzan JF, Liu KB (1995) Late-glacial stage and Holocene tropical ice core records from Huascarán, Peru. Science 269:46–50

Unnerstad L, Hansson M (2001) Simulated airborne particle size distributions over Greenland during Last Glacial Maximum. Geophys Res Lett 28(2):287–290

Vallelonga P, Gabrielli P, Balliana E, Wegner A, Delmonte B, Buretta C, Burton G, Vanhaecke F, Rosman KJR, Hong S, Boutron CF, Cescon P, Barbante C (2010) Lead isotopic compositions in the EPICA Dome C ice core and Southern Hemisphere Potential Source Areas. Quat Sci Rev. doi:10.1016/j.quascirev.2009.06.019

Washington WM, Parkinson CL (2005) An introduction to three-dimensional climate modeling, 2nd edn. University Science Books, Sausalito, California

Weller R, Wöltjen J, Piel C, Resenberg R, Wagenbach D, König-Langlo G, Kriews M (2008) Seasonal variability of crustal and marine trace elements in the aerosol at Neumayer station, Antarctica. Tellus 60B:742–752

Werner M, Tegen I, Harrison SP, Kohfeld KE, Prentice IC, Balkanski Y, Rodhe H, Roelandt C (2002) Seasonal and interannual

variability of the mineral dust cycle under present and glacial climate conditions. J Geophys Res 107(D24):4744. doi:10.1029/2002JD002365

Winckler G, Fischer H (2006) 30,000 years of cosmic dust in Antarctic ice. Science 313:491

Wolff EW, et al (2006) Southern Ocean sea-ice extent, productivity and iron flux over the past eight glacial cycles. Nature 440:23. doi:10.1038/nature04614

Wolff EW, Hall JS, Mulvaney R, Pasteur EC, Wagenbach D, Legrand M (1998) Relationship between chemistry of air, fresh snow and firn cores for aerosol species in coastal Antarctica. J Geophys Res 103(D9):11057–11070

Wurzler S, Reisin TG, Levin Z (2000) Modification of mineral dust particles by cloud processing and subsequent effects on drop size distributions. J Geophys Res 105(D4):4501–4512

Xu J, Hou S, Ren J, Petit J-R (2007) Insoluble dust in a new core from Dome Argus, central East Antarctica. J Glaciol 53(180):154–156

Zárate MA (2003) Loess of southern South America. Quat Sci Rev 22:1987–2006

Zender CS, Bian H, Newman D (2003) Mineral dust entrainment and deposition (DEAD) model: description and 1990s dust climatology. J Geophys Res 108(D14):4416. doi:10.1029/2002JD002775